SEISMIC PERFORMANCE EVALUATION OF REINFORCED HCB FULLY GROUTED MASONRY WALLS AND ITS PERFORMANCE COMPARING WITH UNREINFORCED FULLY GROUTED MASONRY WALLS

MSc THESIS

ZERIHUN TALE BIZUNEH

HAWASSA UNIVERSITY, HAWASSA, ETHIOPIA

APRIL 2021

SEISMIC PERFORMANCE EVALUATION OF REINFORCED HCB FULLY GROUTED MASONRY WALLS AND ITS PERFORMANCE COMPARING WITH UNREINFORCED FULLY GROUTED MASONRY WALLS

ZERIHUN TALE BIZUNEH

A THESIS SUBMITTED TO THE

DEPARTMENT OF CIVIL ENGINEERING

HAWASSA INSTITUTE OF TECHNOLOGY,

SCHOOL OF GRADUATE STUDIES

HAWASSA UNIVERSITY

HAWASSA, ETHIOPIA

IN PARTIAL FULFILLMENT OF THE

REQUIREMENTS FOR THE

DEGREE OF

MASTER OF SCIENCE IN CIVIL ENGINEERING

(SPECIALIZATION: STRUCTURAL ENGINEERING)

APRIL 2021

DECLARATION

I hereby declare that this thesis entitled **“Seismic performance evaluation of reinforced HCB fully grouted masonry walls and its performance comparing with unreinforced fully grouted masonry walls”** was prepared by me, with the guidance of my advisor. The work contained herein is my own except where explicitly stated otherwise in the text, and that this work has not been submitted, in whole or in part, for any other degree or professional qualification.

Name: Zerihun Tale

Signature: ___________________

Date: _______________________

Place: Hawassa, Ethiopia

SCHOOL OF GRADUATE STUDIES

HAWASSA UNIVERSITY

ADVISORS' APPROVAL SHEET

This is to certify that the thesis entitled "**Seismic performance evaluation of reinforced HCB fully grouted masonry walls and its performance comparing with unreinforced fully grouted masonry walls"** submitted in partial fulfillment of the requirements for the degree of Master with specialization in Structural Engineering, the Graduate program of the Department of Civil Engineering, and has been carried out by **Zerihun Tale** Id No PGStru/046/09, under my supervision. Therefore, I recommended that the student has fulfilled the requirements and hence hereby can submit the thesis to the department.

Temesgen Wondmu (PhD)	__________	____________
Name of Major Advisor	Signature	Date
Asnake Kefelegn (MSc)	__________	____________
Name of Co-advisor	Signature	Date

SCHOOL OF GRADUATE STUDIES

HAWASSA UNIVERSITY

EXAMINERS' APPROVAL SHEET

We, the undersigned, members of the board of examiners of the final open defense by **Zerihun Tale,** have read and evaluated his thesis entitled "**Seismic performance evaluation of reinforced HCB fully grouted masonry walls and its performance comparing with unreinforced fully grouted masonry walls**", and examined the candidate. This is, therefore, to certify that the thesis has been accepted in partial fulfillment of the requirements for the degree of Master's of Science in Civil Engineering with Specialization in structural engineering.

Temesgen Wondmu (PhD)	_______________	_____________
Name of Major Advisor	Signature	Date
Surafel Tsegaye (MSc)	_______________	_____________
Name of Internal Examiner I	Signature	Date
Sorasa Belay (Msc)	_______________	_____________
Name of Internal Examiner II	Signature	Date
Binaya Patnaik (PhD)	Binaya Patnaik	_____________
Name of External Examiner	Signature	Date
________________________	_______________	_____________
SGS Approval	Signature	Date

Final approval and acceptance of the thesis is contingent upon the submission of the final copy of the thesis to the School of Graduate studies (SGS) through the Department Graduate Committee (DGC) of candidate's department.

ACKNOWLEDGEMENT

First and foremost, I thank the Almighty God for giving me the strength to endure the challenges in my quest to complete this thesis. Secondly, I am expressing my deepest appreciation to my advisor, Dr. Temesgen Wondmu for his patience, guidance, timely comments & valuable advice throughout the process of completing this thesis.

My heartfelt thanks also go to Co-Advisor Mr. Asnake Kefelegn, for his valuable ideas & comments. And my friends have contributed a big input to attain the objectives of this thesis. Thus, my gratitude goes to all who gave their response, assistance, and suggestions with great cooperation.

Also, I would like to express my profound heartfelt thanks to Hawassa University and Ethiopia Road Authority for allowing me to be a part of this MSc program.

Finally, I am endlessly grateful to my beloved wife Meseret Yabeker for her understanding, endless patience, and encouragement. Also, I am extremely grateful to my family for their unlimited support to complete this research work.

ABBREVIATIONS

$\tilde{\varepsilon}_c^{\,in}$	Inelastic compressive strain of concrete
$\tilde{\varepsilon}_c^{\,pl}$	Plastic compressive strain of concrete
$\tilde{\varepsilon}_t^{\,ck}$	Cracking tensile strain of concrete
$\tilde{\varepsilon}_t^{\,in}$	Inelastic tensile strain of concrete
$\tilde{\varepsilon}_t^{\,pl}$	Plastic tensile strain of concrete
$\overline{\varepsilon_t}$ / $\overline{\varepsilon_1}$	Tensile strain of concrete
ε_c	Compressive strain of concrete
ε_{co}	Compressive strain of concrete at peak stress
ε_{cr}	Cracking strain of concrete at peak stress
ε_{cu}	Ultimate strain of concrete
ε_{oc}^{el}	Elastic compressive strain of concrete
ε_{suk}	Characteristic ultimate strain of steel
ε_{sy}	Yield strain of steel
ω_c	Compressive stiffness recovery of concrete
ω_t	Tensile stiffness recovery of concrete
ACI	American concrete institute
ASCE	American society civil engineers
CAE	Complete Abaqus Environment
CDP	Concrete Damage Plasticity
EC	Euro code
E_{cm}	Secant modules of elasticity of concrete
E_m	Modules of elasticity of mortar
ES EN	Ethiopian standards based on Euro norms
E_S	Modules of elasticity of steel
ESL	Equivalent static load
E_u	Modules of elasticity of masonry unit
f_{ck}	Characteristics compressive strength of concrete
f_{ct}	Characteristics tensile strength of concrete
f_{cu}	Cube compressive strength of concrete
FE	Finite Element

FEA	Finite Element Analysis
FEM	Finite Element Method
f_m	Compressive Strength of Masonry Unit
f_u	Ultimate strength of steel
f_y	Yield Strength of Steel
GL	Gravitational Load
G_m	Shear modulus of mortar
G_u	Shear modulus of masonry units
H	Height of Masonry assemblage
HCB	Hollow concrete block
h_m	Thickness of mortar
h_u	Height of masonry unit
IBC	International Building Code
K_{nn}	Stiffness of masonry joint in the normal direction
K_{ss}	Stiffness of masonry joint in the first shear direction
K_{tt}	Stiffness of masonry joint in the second shear direction
kN	kilo Newton
L	Length of Masonry assemblage
RM	Reinforced Masonry
RMW	Reinforced Masonry wall
URM	Unreinforced Masonry
W1A	Un-filled unreinforced masonry wall aspect ratio 1.39
W1B	Fully grouted unreinforced masonry wall aspect ratio 1.39
W1C	Fully grouted reinforced masonry wall aspect ratio 1.39
W2A	Un-filled unreinforced masonry wall aspect ratio 1.95
W2B	Fully grouted un-reinforced masonry wall aspect ratio 1.95
W2C	Fully grouted reinforced masonry wall aspect ratio 1.95
W3A	Fully grouted reinforced masonry wall aspect ratio 2.23
W3B	Fully grouted un-reinforced masonry wall aspect ratio 2.23
W3C	Fully grouted reinforced masonry wall aspect ratio 2.23
ε	Eccentricity
σ_c / σ_2	Compressive strength of concrete
σ_{cu}	Ultimate compressive stress

σ_t / σ_1	Tensile strength of concrete
ψ	Dilation Angle
Ø	Diameter of reinforcement
Þ	Reinforcement ratio
C/C	Center to center

TABLE OF CONTENTS

LIST OF TABLES

LIST OF FIGURES

ABSTRACT

A reinforced hollow concrete block masonry walls constructed by assembling masonry units, and it was the key structural element widely used to resist lateral loads in masonry buildings. Unreinforced hollow concrete block Masonry wall rapidly fails because of lateral load like an earthquake. Hence this study attempts to evaluate responses of a reinforced and unreinforced fully grouted hollow concrete block masonry wall, select the best walls based on differing their aspect (H/L) ratio, horizontal and vertical reinforcement ratio, and spacing. Also, know the behavior of reinforced and unreinforced fully grouted hollow concrete block masonry wall under lateral load and determine its percentage effectiveness. The study was conducted using finite element ABAQUS software for which a total of 24 masonry wall models were considered. For validation of the finite element method, reinforced masonry walls experimentally worked by M. Hany (2016), and the experimental results compared with the numerically modeled. The comparison of the results indicated that both experimental and numerical results agreed very well. After the validation, the effect of seismic load on reinforced and unreinforced fully grouted hollow concrete block masonry walls investigated by the quasi-static method. The comparison for ultimate load carrying capacity, stiffness degradation, and displacement ductility of each investigation parameter are carried out from the comparative analysis. It was found that the aspect ratio 1.39 wall vertical reinforcement ratio increases from 0.26% to 0.36%, the ultimate strength increase by 15.344% for push and 14.578% for pull direction. And also, the vertical reinforcement spacing increases the Ultimate strength of the wall decrease. The Ultimate shear resistance of the wall is reduced by 17.21% for push and 14.25% for pull direction for in-plane load when the spacing of Ø16 vertical reinforcement increases from 200mm to 400mm. The aspect H/L ratio increase from 1.39 to 1.95 the ultimate strength decrease by 38.15% for push direction and 41.89% for pull direction. Generally, aspect ratio, vertical reinforcement spacing, and vertical reinforcement ratio variation highly influence hollow concrete masonry wall seismic performance relative to horizontal reinforcement.

Key word: Finite Element Simulation, Horizontal reinforcement, Lateral Displacement Masonry wall, Quasi-static, Vertical reinforcement,

1. INTRODUCTION

1.1. Background of the study

An earthquake is a sudden and rapid shaking of the earth caused by the breaking and shifting of rock beneath the earth's surface. This shaking can sometimes cause landslides, flash floods, fires, and tsunamis. Unlike other natural disasters such as hurricanes, there are no specific seasons for earthquakes. During the last time it caused many losses of life, damage of different property and collapse of buildings at a different part of the world, to overcome the effect of an earthquake a seismic code plays a major role. The purpose of this code is to establish minimum requirements to ensure that an event of an earthquake:

I. Human lives are protected.
II. Damage is limited, and.
III. Structures important for civil protection remain operational.

In seismic areas, an engineer should select a type of construction which able to withstand an earthquake and should design earthquake-safe buildings according to seismic design philosophy such as

- ✓ Strength design philosophy – It allows the building to act elastically during an earthquake
- ✓ Capacity design philosophy – It allows the design of the structure in the strength hierarchy of the members with respect to plastic hinge formation.
- ✓ Performance-based design philosophy – The members are designed following their performance during seismic action, and
- ✓ Displacement-based design philosophy – Structures should be designed to achieve a specified performance level defined by drift limits under a specified level of seismic intensity.

Now a day's structures are constructed from different construction materials such as concrete, steel, and both. These materials have different properties

During an earthquake, the masonry wall of structures is easily damaged, because the masonry or unreinforced masonry wall is weak in tension. Masonry is one of the oldest forms of construction known to humans. The term masonry refers generally to brick, tile, stone, concrete block, etc., or a combination thereof, bonded with mortar. However, many different definitions of masonry are in vogue. The International Building Code (IBC 2009) defines masonry as a built-up construction or combination of building units or materials of clay, shale, concrete, glass, gypsum, stone, or another approved unit bond together with or without mortar or grout or other accepted methods of joining. ASTM E631 defines masonry as construction usually in the mortar natural building stone or manufactured units such as brick, concrete block, adobe, glass, block tile, manufacture stone, or gypsum block. A commonality in these various definitions is that masonry essentially is an assemblage of individual units which may be the same or different kind and bonded together in some way to perform the intended function. From structural engineering, perspective masonry classified as plain or unreinforced masonry and reinforced masonry. Plain masonry refers to construction from natural or manufactured building units of burned clay, concrete, stone, glass, gypsum, or other similar building units or a combination thereof, made to be bonded together, cementitious agent. The strength of plain masonry depends primarily on the high compressive strength of masonry units. Plain masonry, like plain concrete, possesses little tensile strength. This indicates the seismic effect on masonry is very high. But this effect is minimized by adding the tensile reinforcement in the wall along the transverse and longitudinal direction of the wall resists the tensile and compression loading effect, called a reinforced masonry wall. Plain masonry is strong with reinforcement materials such as steel bars, which greatly enhance the tensile and compressive strength of masonry walls. Stated reinforced masonry construction is “masonry construction in which reinforcement acting in conjunction with the masonry is used to resist forces. Mortar keeps concrete masonry units apart and keeps them together at the same time. Generally, the mortar thickness between units is about 9.5 mm, but it could be modified to make room for concrete masonry dimension variations. Moreover, mortar holds concrete masonry units together by developing a bond between them through which flexural and direct tensile strength produced. The tensile strength might not be significant in reinforced concrete masonry as in unreinforced masonry; nonetheless, it is still crucial for the wall. A horizontal joint was called a bed joint. It is laid in the face shell, and mortar is placed on the face shell only, not the webs. Furthermore, vertical joints are called head joints, mortar is poured into the head joints to a depth equal to the thickness of the face shell on both sides of the wall. Masonry cement is a mixture of Portland or other cement, plasticizing, fillers agents, and other materials intended to improve the mortar achievement. Cement-lime mortar is composed of blending cement such as Portland cement or blended cement, hydrated lime, sand, water, and sometimes admixtures. Every civil structure must be designed for seismic load structures to resist such seismic load structural systems, and components play an important role.

1.1.1. Masonry structure in earthquake engineering

Masonry structures are weak in an earthquake easy fail relative to other building structural components. Masonry structures are considered problematic in earthquake engineering, for example, the complications of any kinds of masonry structure under cyclic loads and the lack of clear strategy for modeling masonry systems. Because of the broader use of steel and reinforced concrete in modern earthquake-resistant construction, researchers have spent most of their attention on these structural systems.

According to Mahmoud N. (2005), masonry systems have many advantages over other competitive systems, such as concrete, precast, and steel under compressive forces have the following benefits.

- Design flexibility with colors, textures, and shapes
- Material that allows designers to build a project that can blend in to and highlight the strength of community
- Durability
- Low maintenance
- Acoustics
- Energy saving
- Fire resistance
- Mold resistance
- Speed and ease of construction etc.

1.2. Statement of the problem

An earthquake load is one cause of the damage of structure, this type of structural damage is starting from the weak part of the structure or the unreinforced walls because unreinforced masonry walls, like plain concrete, possess little tensile strength. Therefore, it cannot use as an efficient building material for structures or structural elements that must resist tensile forces. But reinforced HCB fully grouted masonry wall is highly resisting tensile force because this wall has steel reinforcement. The poor tensile strength of plain masonry makes it unsuitable for horizontal spanning structural elements such as beams and slabs, which resist loads in flexure and thereby are subject to tensile stresses. Due to this reason, unreinforced masonry walls were strong by adding reinforcing materials (steel bars) to increase both its tensile as well as the compressive strength of walls, this forms of masonry construction refer to as reinforced masonry walls. Many researchers conducted the seismic performance of the structural components, like a beam, column, shear wall, and slab, etc., to show that the wall easily and rapidly fails by the seismic load relative to other parts of structures found in seismic zones. So, it better to construct the walls by adding reinforcement (steel bars) in masonry walls called reinforced masonry walls to minimize the damage to the walls. And also, compare the reinforced and unreinforced fully grouted hollow concrete block masonry walls under seismic load and percentage effectiveness of walls the highly resist the seismic load.

1.3. Objective of the study

1.3.1. General objective

The general objective of this thesis was to investigate the behavior of reinforced and unreinforced fully grouted hollow concrete block masonry walls under seismic load by using finite element analysis software ABAQUS (2016)

1.3.2. Specific objectives

- To develop the finite element model of reinforced and unreinforced Hollow concrete masonry wall simulation under seismic load using ABAQUS (2016).
- To investigate the seismic performance of reinforced and unreinforced fully grouted Hollow concrete block masonry wall based on changing aspect (H/L) ratio.
- Compare the lateral displacement versus lateral ultimate load response of reinforced fully grouted HCB masonry and unreinforced fully grouted HCB masonry walls.

- To investigate the behavior of reinforced fully grouted HCB masonry walls by changing their horizontal and vertical reinforcement ratio of masonry under lateral load.

1.4. Research questions

- How to model reinforced and unreinforced Hollow concrete masonry on finite element software ABAQUS?
- How does reinforcement use in hollow concrete block masonry walls affect the seismic performance relative to an unreinforced fully grouted hollow concrete block masonry walls?
- How do aspect ratio (H/L) and reinforcement spacing either lateral or longitudinal direction affect the seismic performance of reinforced fully grouted hollow concrete block masonry walls?

1.5. Scope and limitation of the Study

In this study, the analysis was performed using (21) reinforced and (3) unreinforced fully grouted hollow concrete block masonry walls. The effect of an earthquake on reinforced HCB fully grouted and unreinforced HCB fully grouted masonry wall building subjected by a seismic load on earthquake-affected site in Ethiopia. Besides concerned about the behavior of reinforced HCB fully grouted masonry and unreinforced HCB fully grouted buildings panel wall subject to seismic loading using finite element analysis software. The analysis was carried for a 3D wall single panel wall subjected to earth quack load on the reinforced and unreinforced fully grouted masonry wall building.

In this study cyclic quasi-static loading was used on reinforced HCB fully grouted masonry walls and unreinforced HCB fully grouted masonry wall. Additionally, in this study, all model was a single panel masonry, because the modeling of multi-panel masonry is difficult as a result of the capacity and longer running time of the available computer.

1.6. Research Organization

This research encompasses six chapters. The first chapter was an introduction part; it covers general information about the behavior of reinforced and unreinforced masonry walls to earthquake load. In addition to this: the objective, statement of the problem, and limitation of the research have stated in this chapter, sufficient information, and guidance regarding effects of seismic or earthquake load on reinforced and unreinforced masonry wall as literature review which has presented under chapter two. Chapter three deals with Finite Element analysis of reinforced HCB fully grouted masonry wall and unreinforced HCB fully grouted masonry wall subjected to seismic load using ABAQUS / CAE; additionally detailed information and procedures about ABAQUS simulations.

Chapter four deals with validation of reinforced concrete beam using Finite Element analysis of subjected to impact load using ABAQUS / CAE. Output results obtained from ABAQUS, such as lateral load versus lateral displacement have a good agreement with experimental data.

Results and the discussion analytical simulation of reinforced HCB fully grouted masonry wall and unreinforced HCB fully grouted masonry wall subjected to seismic load using ABAQUS and discussions are presented under chapter five and finally conclusion and recommendations for further studies.

2. LITERATURE REVIEW

2.1. Introduction

A reinforced hollow concrete block masonry wall was constructed by assembling masonry units for example concrete blocks or bricks, mortars, reinforcing, and sometimes grout that is a kind of soupy concrete.

2.1.1. Types of Concrete Blocks or Concrete Masonry Units

Depending upon the structure, shape, size, and manufacturing processes concrete blocks are mainly classified into two types and they are

a. Solid Concrete blocks
b. Hollow Concrete Blocks

2.1.1.1. Solid Concrete Blocks

Solid concrete blocks are commonly used, which are heavyweight and manufactured from the dense aggregate. They are stronger and provide good stability to the structures. So for large work of masonry like for load-bearing walls these solid blocks are preferable. They are available in large sizes compared to bricks. So, it takes less time to construct concrete masonry than brick masonry.

Figure 2-1 Solid concrete blocks

2.1.1.2. Hollow Concrete Blocks

Hollow concrete blocks contain void areas greater than 25% of gross area. The solid areas of hollow bricks should be more than 50%. The Hollow part may be dividing into several components based on our requirements. They are manufactured from lightweight aggregates. They are lightweight blocks and easy to install.

2.1.2. Properties of Mortar for Reinforced Concrete Masonry Walls

Mortar keeps concrete masonry units apart and keeps them together at the same time. Generally, the mortar thickness between units was about 9.5 mm but it could be modified to make rooms for concrete masonry dimension variations, in this way mortar keeps units apart. Moreover, mortar holds concrete masonry units together by developing a bond between them through which flexural and direct tensile strength is produced. The tensile strength might not be significant in reinforced concrete masonry as in unreinforced masonry; nonetheless, it is still crucial for the wall.

A horizontal joint, which is called bed joint, is laid in the face shell and mortar is placed on the face shell only not the webs. Furthermore, vertical joints are called head joints, and mortar is poured into the head joints to a depth equal to the thickness of the face shell on both sides of the wall. Both head joint and bed joint can be seen from Figure 2-2.

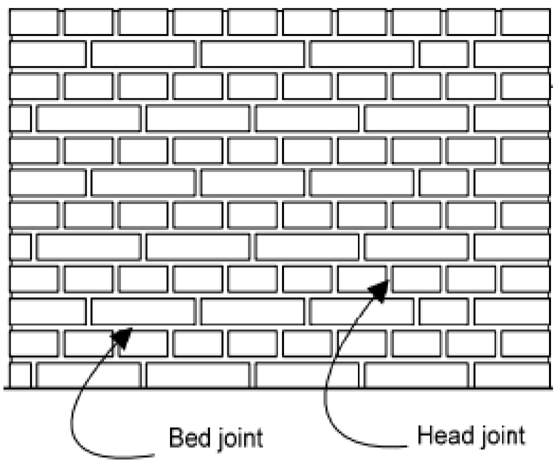

Figure 2-2 Masonry unit arrangements and joint masonry structure (Ludovikus S.(2007))

Mortars are mixtures of plastic binder resulting from the combination of sand and water with cementing material that may be cement, lime, or a mixture of both materials. Their main properties are compressive-tensile strength, elasticity, and the ability to avoid water absorption. ASTM C 270 classified mortars into M, S, N, O types and the strongest type is M then others respectively. The type of mortar used in the construction of the majority of a reinforced masonry wall is either Type S or Type N. additionally, Type S or Type M is applied in the seismic category D or higher.

Finally, mortars are classified by either proportion or by property, not both. Categorizing mortars by proportion was a default in the case the designer does not determine the mortar classification

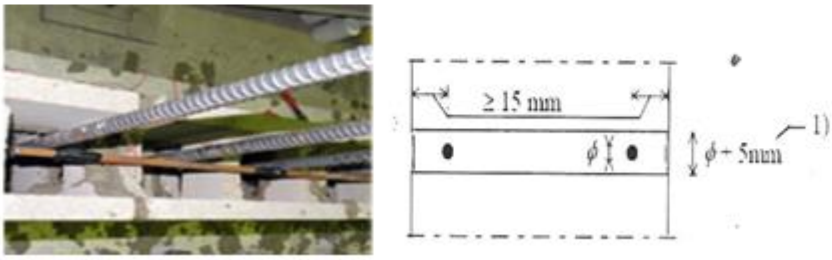

Figure 2-3 Reinforcement detail in study wall (Heny M. et al (2017) and ES: EN 6 1996:2015 part 1)

A reinforced concrete masonry wall was constructed by assembling masonry units for example concrete blocks or bricks, mortars, reinforcing, and sometimes grout that is a kind of soupy concrete.

Figure 2-4 Detail of RM wall (Hany Mohamed Seif Eldin (2016))

The shear wall was a structural member used to resist lateral forces, i.e. parallel to the plane of the wall. For slender walls where the bending deformation is more, the Shear wall resists the loads due to Cantilever Action. In other words, Shear walls are vertical elements of the horizontal force resisting system. Wall is less stiff to resist earthquake because of lack of tensile resistance. Nowadays many researchers have conducted many studies on the seismic effect of different types of walling systems.

Seif ElDin H. M and Galal K (2018) studied the effect of reinforcement anchorage end detail and spacing on seismic performance of reinforced masonry shear walls. This paper investigated the in-plane seismic performance of fully grouted reinforced masonry shear walls dominated by shear-flexure failure. This experiment work involved assessing the response of the five single-story reinforced masonry shear walls when subjected to in-plane axial compressive stress and cyclic lateral excitations. The model parameters were the horizontal reinforcement anchorage end detail and the spacing of the horizontal and vertical reinforcement. The research model examined three anchorage and details 180ºstandard hook, 90º hook, and straight. Also, the vertical spacing of the horizontal reinforcement (400 and 800) and two horizontal spacing of vertical reinforcement are used (200mm and 800mm). All the tested reinforced masonry walls had the same dimension 1.8m*1.6m*0.19m and conducted with a constant horizontal reinforcement ratio of 0.13%, also the masonry unit nominal dimensions of 390mm*190mm*190mm, the wall was constructed on reinforced concrete (RC) foundation with dimensions of 2.3m*0.64m*0.45m and were taste under a constant axial compressive stress of 1.0MPa, use bars 10m@400mm.the test result 180º standard hook was the most efficient in terms of straight and the ductility with a slight difference in the strength and 15% higher ductility than using the straight walls. In-wall that was conducted with closely spaced reinforcement was able to reach 15% and 80% higher strength and ductility than similar walls with large spacing when using the same reinforcement ratio. Consequently, the trend of damping for a structural element such as the shear wall, with respect to the top drift or the displacement ductility can provide an indication of the overall response of reinforced masonry structures. Generally, the spacing of horizontal and vertical reinforcement shows a significant impact on the total energy dissipated by tested reinforced masonry walls under in-plane cyclic lateral excitations. To compare the end detailing reinforcement of wall 90^0

is high shear strength than 180^0 hook of reinforcement and displacement ductility 180^0 higher than displacement ductility of 90^0 hook reinforcement.

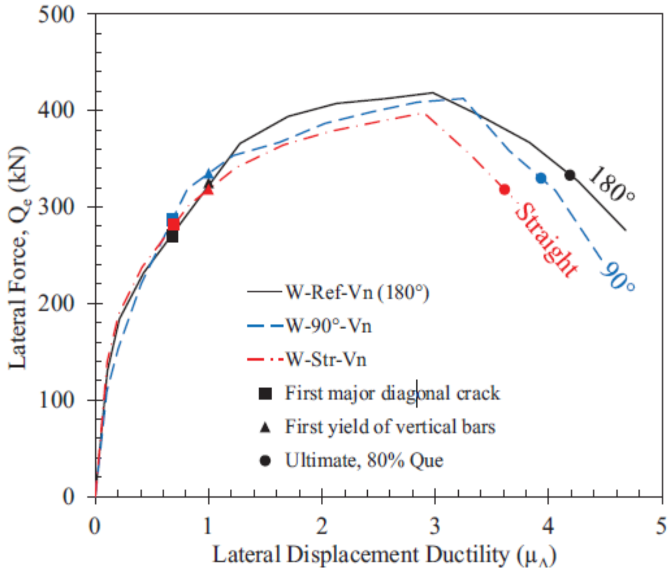

Figure 2-5 Effect of horizontal reinforcement anchorage end detail on in-plane shear strength of RM walls

Tomazevic and Weiss (1994) studied the seismic behavior of two three-story, plain, and reinforced masonry building models with identical structural configurations. The measured response and observed mechanism of the structural behavior have been using to analyze the load-bearing and energy- dissipation capacity of each structural type. They concluded that, if the walls are not reinforced, the flexural capacity of their sections below and above the slab is too low to activate the flexural capacity of horizontal structural elements. Cracking between walls and slab occurs, indicating the pier action of the walls and story mechanism of the building at the ultimate state. If reinforced, the structural walls behave like vertical cantilevers coupled with horizontal structural elements. The distribution of bending moments induced in the walls by seismic loads depends on the rigidity of the wall and horizontal element.

Sayed and shrive (1996) develop a nonlinear elasto-plastic finite element model for face-shell bedded hollow masonry using is parametric shell elements. The nonlinear behavior of the masonry in compression due to progressive cracking and geometric and materially nonlinear behavior of the masonry in the model details of the elasto-plastic constitutive model and failure criteria of both blocks and mortar joints were presented. Results from a simulated test of a three-block high prism were given in the form of stress, strain and displacement plots. The behavior of the model was compared to known experimental behavior. The modeled specimens gave lower loads than those obtained experimentally because the full extent of mortar crushing and the final buckling out of the face- shells was not modeled

Also, investigate the response of confined concrete masonry wall subjected to in-plane cyclic load by A.lcroz O. et al. (2018). The paper aimed to know the behavior of reinforced masonry walls made with multi-perforated concrete units subjected to reverse cyclic lateral load. This experimental research investigated six fully confined masonry walls made with multi-perforated concrete units that were subjected to reversal cyclic lateral loads. The only variable investigated was the amount of joint reinforcement. All other variable was fixed; the height to length aspect ratio (H/L) was set one. The reinforced steel bars placed in the bad joints every two courses, consisted of small diameter bars with nominal yielding stress 588MPa. Numerous strain gages were installed on the rebar to monitor deformation and subsequently estimate the lateral strength contributed by the reinforcement. The strength due to the masonry was estimated at the difference between the total lateral strength and the strength attributed to reinforcement.

In this model, there are used two types of reinforcement in masonry walls one provided with in the bed joints. However, bond beams are not used in confined masonry walls. Also, joint reinforcement (JR) is providing in the masonry walls takes the form of a ladder or truss-like welding wires. Although the purpose of joint reinforcement (JR) for cracking control against volumetric changes in a masonry wall or bonding of multiple Wythe’s, it is also used as shear reinforcement the comparison of the seismic performance of full grouted reinforced walls with bond beams and walls with joint reinforcement showed that walls using joint reinforcement had more uniformly distributed damage and higher lateral resistance.

This sample used three diameters of wire (3.97mm, 6.76mm, and 6.35mm) fit in the mortal joints. This weir should be properly anchored in the tie, columns, or internal cells. Lapping is not allowed as the bond between the wire and mortal, and between the mortal and masonry units, degrades cracking based on their code joint reinforcement seismic reduction factor is 2. This research is conducted by using masonry units 120mm*120mm*240mm multi-perforated concrete blocks. And joint reinforcement is placed every two courses, with a vertical spacing of 200mm, the wires were anchored in the tie-column with 90-degree standard hooks.

The dimension and amount of joint reinforcement are different. Tie-columns longitudinal reinforcement 4Ø19mm bars. And also f_c is 24.5MPa for concrete, for tie-column, beam and slab. Based on this sample the experimental result the displacement increases with increase area of steel. Ductility at failure shows a small increase with the amount of reinforcement, however at peak strength show on the increase. Generally, this research shows the ductility displacement behavior of confined masonry walls by adding joint reinforcement. The result shows that the contributions of the reinforcement to the lateral strength increase with the amount of reinforcement to a certain limit and that the contribution of masonry decreases.

L. Avila, G.V et al. (2018) studied the response analysis of concrete block masonry wall building: an experimental study using shaking table. Based on this paper concrete masonry block is the study indicates that despite the same seismic inputs were applied to both models the final state of UM building and its nonlinear behavior led to a considerable amplification of the deformations and damages. For this model was clear the in-plane shear mechanism was developed. Consecutive tests increase rapidly the horizontal cracks and the loss of connection between structural elements through the high of the model. It is also concluded that the combination of vertical and horizontal reinforcement, about the minimum required by Euro-code 8 improves the seismic response of concrete block masonry buildings, leading to adequate structural robustness for very high seismic loading. It is believed as well that the behavior through the tests was influenced by the mortar vertical joints in which the steel reinforcement was placed. The results confirm the adequacy of modern unreinforced masonry by using a traditional bond pattern, with robust units, to withstand seismic loading, as not damage was presented after an input of 0.25g and not collapse after input of 1.33g.

Khalaf et al. (1994) studied the effect of the strength of concrete infill and mortar joint type on the compressive strength and behavior of unfilled and filled fully and half- block prisms compressed normal to the bed face. They reached the following conclusion:

- The strength of both the full and half single block high specimens increased as the strength of the concrete infill increased.
- Removing the mortar joint produces a large reduction in filled prism strength (a 10mm polystyrene joint was used instead). Based on the gross area of the prism with polystyrene joint, the contribution of the concrete infill to the strength of full and half block prism was found to be 25%.
- The presence of concrete infill significantly reduced the compressive strength of both full- and half-block prisms, with mortar joints or with plaster joints, compared to values for un-fill prisms. With only one exception, the best compressive strength results were achieved when the deformation characteristics of the infill matched those of the concrete block. This was achieved by using concrete infill with a cube compressive strength of 45% to 50% higher than that of the concrete block.

Songbo li and Anton N. Fried (1994) are analyses for seismic behavior of reinforced masonry walls. This research describes the failure process of unreinforced and reinforced masonry walls with lower levels of reinforcement and lower mortal grades under seismic loading and also discusses the possible forms of reinforcement for masonry walls and their effects. Based on these results and the results from other researchers, this study will examine the structural behavior and methods of designing clay brick walls with low reinforcement ratios under seismic loadings. Reinforcement usually does not change the initial crack load of masonry walls. Indeed, a wall's initial crack is controlled by many factors, such as the grade of mortar, the rigidity of the masonry wall, the vertical load on the wall, etc. Steel bars become effective only after the initial crack has occurred. The position of the initial crack and consequently the subsequent distribution of loads in a wall are reasonably random because of the variations in the material properties.

Then the initial crack will originate somewhere in this element if the wall is under bi-directional stresses. Therefore, this element will not maintain its stiffness. The consequent redistribution of load will result in neighboring elements bearing extra forces. Causing horizontal crack and tensile forces to develop in element with the potential for crack. That in the masonry wall the cracks will gradually develop in the diagonal directions after the initial crack forms, with the wall will finally losing its load-bearing capacity. But a reinforced masonry wall will behave differently. Horizontal bars will bind the masonry elements together and reduce the relative displacement between cracked parts in a cracked element Neighboring element will not bear the extra forces from the cracked elements because the steel bars which are stronger than masonry materials in tension will distribute these additional loads away.

Consequently, the reinforced element will no longer be the weakest one after the initial crack occurs and other weaker elements will crack resulting in the steel bars in their locality distributing extra loads away from the cracked element. Through this process, there will be a distribution of cracks over the entire wall, the precise pattern depending on the arrangement of the reinforcement and the actual location of weak elements. Almost all parts of the masonry wall will contribute to the wall's load-bearing capacity unlike in unreinforced walls. The strength of reinforced masonry is not increased with reinforcement but the reinforcement enables the entire wall to be utilized in bearing the load.

Consequently, the strength of the reinforcement is not usually critical; its correct placement and distribution being far more important. Under horizontal cyclic loads, compressively loaded parts of masonry walls may be broken due to the combined effects of bending moment, shear, and compressive forces. The compressive failure of masonry is usually by vertical cracking because horizontal strains are too large. In horizontally reinforced masonry walls the horizontal reinforcement will limit strain in that direction and consequently, an enhancement in the vertical load capacity of walls can be expected. Placing horizontal meshes of reinforcement in walls will result in vertical load enhancement.

However, when horizontal reinforcement is provided by occasional horizontal ties, the masonry between the ties will not gain any enhancement to its vertical load capacity. Horizontal bars placed in slots in bricks may provide vertical planes of weakness at the slots in the masonry and are unlikely to benefit the vertical load-carrying capacity of walls. The result shows the relationship between the strengthening effect of reinforcement and the reinforced ratio is not linear, however, the strength will continue to increase along with the increase of reinforcement ratio.

This means the result would be very dangerous since we know the increase of the strength is not true. The load-bearing capacity of masonry structures under seismic conditions can be improved by using relatively minor amounts of reinforcement. The crack patterns of masonry walls at failure can be altered by the addition of reinforcement. The reinforcement redistributes load resulting in all the masonry elements contributed to the wall strength unlike in a reinforced wall where only a few unit's contributions to the wall's capacity. Based on this paper test results determine the shear strength of clay brick masonry walls under seismic loading. It suggests that reinforced masonry walls have better seismic behavior not because the material strength has been increased after reinforcing by steel bars, but because the full-strength potential of the masonry is brought into full play. Therefore, the strength of reinforcement is not such an important property but of more importance is the correct positioning and distribution of the steel bars on masonry walls.

Ehsani et al. (1997) studied the shear behavior of unreinforced masonry retrofitted with FRP overlays. The study included 37 clay brick specimens with FRP overlays. Three different fabric densities were used and the fiber orientation, as well as the fabric length, was varied to observe their effect on the developed strength. Two modes of failure were observed: (1) shear failure along the bed joint [Figure 2.6]; and (2) delamination of fabric at the middle-brick region or fabric edges. The type of failure was influenced by the fabric strength. The strength and stiffness of the specimens were highly influenced by the fiber orientation. Changing the fiber orientation from 90° to 45° led to a slight increase in the ultimate load

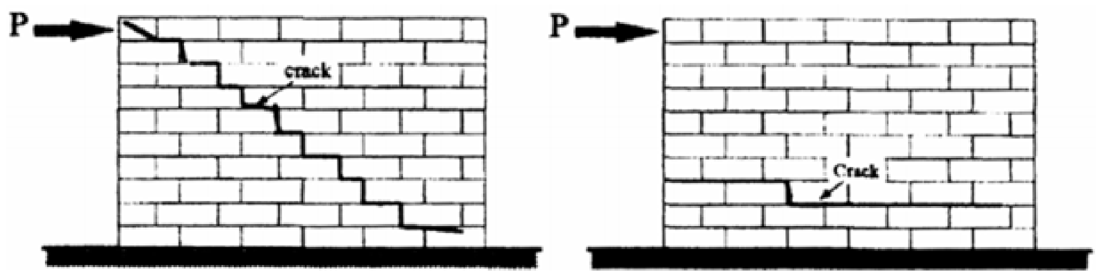

(a) (b)

Figure 2-6 Models of failure in URM wall subjected to lateral load P (a), Diagonal tension; (b), Slip along bed joint (Ehsani et al. (1997))

WeifanXu, Xu yang and Fenglai Wang (2018) also study the experimental investigation on the seismic behavior of newly-developed precast reinforced concrete block walls. Masonry structures have the advantage of reducing construction cost and improving construction efficiency. Additionally reinforced masonry wall exhibit better seismic performance compared to traditional unreinforced masonry walls. In this study a research program was conducted to newly-develop precast reinforced masonry walls were designed and failure-tested under lateral cyclic loading. This test was conducted by using four samples of spacemen who had a high aspect ratio and the same conflagration which was 1390mm*3200mm*190mm (length*height*width). It should be noted that the two courses at the top of each spaceman were used for load transfer only. Therefore, the effective wall height is 2800mm and the corresponding aspect ratio was 2 for all specimens. In this sample two masonry walls constructed by traditional technology and two masonry walls is precast masonry walls had used, reinforcement of all traditional and precast walls identical except that the vertical rebar of precast walls extended to the full height of the walls while lap joints were used for the vertical steel connections at the bottom region of the traditional reinforced masonry walls through cleaning holes. The vertical reinforcement was with five steel, bars of diameter 14mm which were placed at each of the two side calls and the middle call of the specimen.

And also use horizontal reinforcement was with two steel bars of diameter 12mm and spacing of 200mm. the reinforcement of the specimens was selected according to the Chinese code. The horizontal and vertical reinforcement ratios of all walls were 0.60% and 0.29% which satisfies the minimum ratios of the reinforcement masonry. Also the dimension of full and half blocks used in the research 390mm*190mm*190mm and 190mm*190mm*190mm respectively. From the experimental result the crack patterns of the specimens under cyclic loading. In general, both traditional and precast masonry test walls exhibited a similar typical flexural failure mode even though some differences existed in the damage progression. During the test horizontal cracks initially appeared in the bad joints at the base of the walls as loading continued. The length and width of horizontal cracks tended to increase, which led to the translation of the natural axis the reduction of the compression zone depth and increase compression stress, and also strains of the vertical rebar developed significantly, which manifested its effective role in bearing the tensile stresses due to flexure, with the increase due to flexure. With the increase of the imposed lateral displacement, vertical splitting cracks formed in blocks at the corner. The strain gauges showed that the vertical rebar at the sides of the specimen yielded at this stage crushing at the corner.

Also, displacement ductility is a measurement of the ability of the shear will to deform in the elastoplastic stage without significant degradation of strength. In this study ductility defined as the ratio between the top displacement in the past-peak stage and the yielding point of the test, a wall was determined according to the energy method. Generally, this research, precast construction technology was introduced to overcome these shortcomings. Quasi-static tests on two traditional and two precast fully grouted reinforced masonry wall, were conducted the results showed that the flexural capacity of precast walls exhibited about 10% increase when compared to traditional reinforced masonry walls, also under the same axial compression precast reinforced masonry walls that failed in flexural mode showed favorable deformation capacity and displacement ductility value corresponding to 15% strength degradation reached 4.9. Therefore, this experiment suggests the precast reinforced masonry walls have satisfactory seismic performance.

Angigu.et al. (2017) also investigates experimental study and parameter analysis on the seismic performance self-centering hybrid reinforced concrete shear wall. Reinforced concrete (RC) shear walls are a common and cost-effective way of providing lateral force resistance to buildings in seismic areas around the world. Conventional RC shear walls are properly designed to have a nonlinear response under design level earthquakes in order to absorb input earthquake energy, which leads to significant residual drift and damage accumulated at the wall base plastic hinge region after the earthquake. In recent years, researchers studied the seismic behavior of the self-centering shear walls and self-centering hybrid shear walls, analytically and experimentally.

Kurama proposed a self-centering shear wall with bonded steels at the horizontal joints and a corresponding design method, and analyzed original buildings incorporating these types of self-centering hybrid shear walls in different seismic zones. The total height of each specimen was 4.2 m, and the length and width were 1.5 and 0.2 m, respectively. Each specimen had two joints, one at the middle of the wall, the other at the wall base. In each specimen, the longitudinal reinforcement at joints was spliced by grouted sleeves manufactured by Beijing SidaJianmao Technology Development Company. The grouted sleeves have a threaded connection at one end and a grouted connection at the other end. The materials used in these cyclic loading tests. The lateral load applied to the specimens was supplied through the use of a hydraulic actuator. This actuator is bolted to the reaction wall at a height of 4m from the strong floor. Gravity load was simulated via three hydraulic jacks situated at the top surface of each specimen. An axial load of 900 KN was provided by the three hydraulic jacks. Ball bearings attaching the hydraulic jacks to the steel beam allow the hydraulic jacks to translate with the specimen during the tests. In this section, the performance of both specimens during the cyclic loading test is presented and compared. Shear wall was performed as a precast shear wall with a sliding effect observed during the loading test. The sliding effect was induced by the grouted sleeves connections. Other walls displayed a better deformation ability and self-centering ability. Because of the variation of gravity load, the hysteretic behavior was not of the typical flag-shaped type.

2.2. The failure mode of masonry wall due to lateral load

According to Marzhan, G. (1998) Failure of masonry walls can occur: based on this research masonry walls subjected by lateral load failure of wall Due to In-Plane Action, and Due to Out-of-Plane Action.

2.2.1. Failure Due to In-Plane Action

The walls with in-plane action may collapse in three main failure modes: sliding, flexural, and shear; Figure 2-6 shows details. Sliding failure is defined as the horizontal movement of entire parts of the wall on the single HCB layer, vapor barrier, or mortar bed. Flexural failure, where the wall behaves as a vertical cantilever under lateral bending and, either cracking in the masonry tension zone (opening of bed joints) or crushing at the wall toe will limit the bearing capacity. Shear failure is characterized by a critical combination of principal tensile and compressive stresses as a result of applying combined shear and compression are leads to typical diagonal cracks. In practice mainly two types of shear cracking can be observed, joint cracking by local sliding along the bed

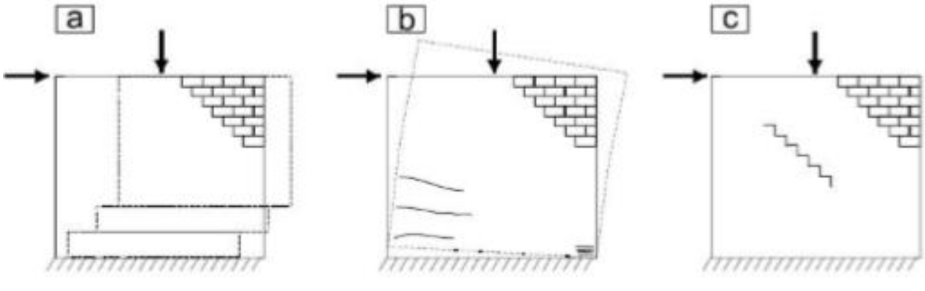

Figure 2-7 Different types of failure modes in masonry walls with in-plane action: (a) Sliding Failure, (b) Flexural Failure, (c) Shear Failure (Marzhan, G.,1998)

2.3. Review on FEM Simulation of masonry walls

Modeling of masonry wall techniques in finite element software was different based on accuracy and detail required. According to K.F. Abdulla et al. (2017), FEM for masonry is based on three main modeling approaches. The choice depending on the level of accuracy and detail required.

a) Micro modeling, in which thickness of mortar and brick/unit both are considered and analysis is carried out. As it is more accurate but difficult to model and time-consuming.
b) The simplified micro modeling approach, in this modeling is simple then micro modeling and thicknesses of mortar are not visualized as unit thickness interface is provided between units/bricks.
c) Macro modeling, in this whole wall, is considered homogeneous and it is the fastest way to analyze the wall but results and not accurate as observed.

Generally with relative to these three types of masonry modeling approaches the detail micro model can provide accurate results.

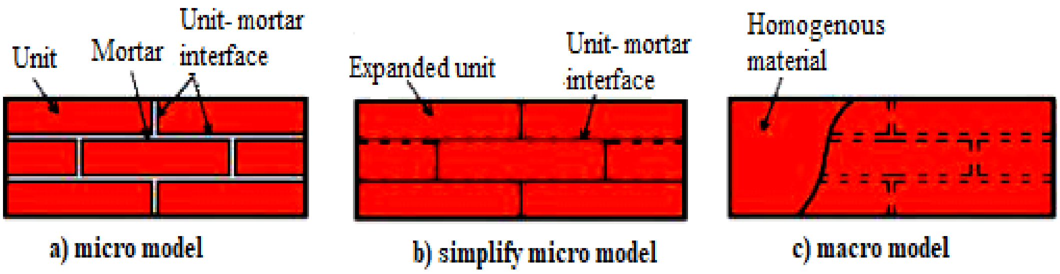

Figure 2-8 Numerical masonry wall model approach (K.F. Abdulla et al, 2017).

Based on B. H. Al-Gohi, et al., 2013 in the last two decades, numerical procedures in engineering have been developed tremendously and more attention has been given by researchers to develop numerical methods to simulate the real behavior of masonry structures. However, many factors influence the structural behavior of masonry walls, such as geometry, anisotropy of the units, bond properties, material properties of units and mortar, and workmanship, which make the numerical simulation of masonry extremely. Nevertheless, masonry researchers have attempted to model masonry behavior through numerical trials and they were successful to get the real behavior of masonry to acceptable levels.

Under the research conducted by Bolhassani et al. 2015, the masonry modeling technique was either micro or macro. The macro modeling endeavors to define the masonry based on the homogeneous material and, it can provide an approximate response only equivalent to a single material, which is an assemblage of units and mortar with average properties. The micro model represents the actual pattern of masonry and considers the masonry units mortar and interface separately, each is characterized by distinct properties. Micro modeling studies are required to get a better understanding of the local behavior of masonry structures. The necessary parameters for modeling have to be extracted from small-scale laboratory tests. On the other hand, macro modeling is relevant for the global analysis of masonry structures, where the structure is composed of walls with sufficiently large dimensions. Bolhassani et al, 2015 also modeled masonry walls subjected to uniaxial and diagonal compression load in an ABAQUS environment. Hollow and partially grouted masonry were modeled using detailed micro-modeling. Mortar joints and units were smeared into one homogeneous material, and they were modeled using the concrete damage plasticity (CDP) model available in the ABAQUS library. The joint was modeled as an interface cohesive element with traction–separation behavior. Based on the concluded results, the more accurate response of masonry can be represented by the detailed micro modeling which showed good agreement to the experimental tests in the difference of behavior and strength of partially and fully grouted masonry.

Zhuge et al. (1998) develop a comprehensive analytical model studying the response of unreinforced masonry to in-plane dynamic loading, including earthquake loads. The analysis was implemented in a nonlinear finite element program. Masonry was treated as a nonlinear homogeneous orthotropic material. A failure envelope was also developed that was capable of predicting both joint sliding and cracking and/or crushing types of failure. The effect of bed joint orientation was considered; this was achieved through a ubiquitous joint model. The model is capable of performing both static and time history analyses of the masonry structure. Nonlinear 19 dynamic analyses were carried out using the modified newton- raphson iteration scheme in conjunction with the new mark time integration algorithm. To calibrate the model and to demonstrate its applications, several numerical examples were treated, and the results were compared with those from full-scaled tests on masonry shear walls under both cyclic and dynamic loads. The conclusion was that the nonlinear behavior of masonry is caused by two major effects progressive local failure (cracking of mortar) and nonlinear deformation characteristics (in the biaxial compression and uniaxial compression stress state). All these effects were considered in the orthotropic constitutive relations developed in this research. A failure envelope was developed that was capable of predicting both joint sliding and cracking and/ or crushing types of failure for a homogeneous material model. The effect of bed joint orientation was considered. A simple secant-type unloading/ reloading curve was adopted for masonry under tension, and the unloading parameter was determined by calibrating the finite element model against experimental results. The analytical model was validated by comparing results with various experimental results, and reasonably good agreement was found. However, further research could improve the model.

2.4. Summary on seismic resistance and modeling technique of masonry structure

The above literature shows only on general building seismic resistance, detailed the journals to focus on an unreinforced masonry wall. The conclusion of many journals masonry wall the seismic resistance of vary little, and masonry wall masonry is modeled on FEM based on three main modeling approaches namely, micro modeling, simplify micro modeling, and macro modeling, But simplify micro model accurate result of analysis than others. Based on the above literature review presented, the following are some of the key knowledge gaps that require further works.

- For most numerical analysis, 3-D of reinforced masonry wall under seismic load is not detailed identification. The many kinds of research on masonry structure worked by experimentally not detail work by numerical or analytical method.
- Many kinds of research do not show clear techniques to increase or improve the strength of masonry structures under seismic load. The seismic performance of masonry walls does not have a clear conclusion in any journal.
- For the above literature modeling of masonry on finite element more focus on an unreinforced masonry wall. Not show clearly the modeling technique of full grouted reinforced masonry wall.

3. MATERIALS AND METHODOLOGY

This chapter describes the different shapes of elements used to develop the model. As well as techniques and tools to establish the boundary conditions and load protocol of unfilled, unreinforced HCB fully grouted and reinforced HCB fully grouted masonry walls. The aspect ratio (H/L) are 1.39 1.95 and 2.23.

3.1. General

As mentioned earlier the primary goal of this study was the analysis of the seismic performance of an unreinforced HCB fully grouted and reinforced HCB fully grouted masonry walls by using a finite element with the different parametric study. This chapter is dedicated to describing the FE method and modeling of material properties, for concrete block (HCB) masonry longitudinal and bed joint mortar grouted concrete fill and rebar. The computational simulation program was a 3D finite element analysis program called ABAQUS Version 6.16 and more specifically, it has done according to ABAQUS, 6.16 documentation guidelines.

ABAQUS /CAE, 2016 is a general-purpose powerful engineering simulation tool and can solve a wide range of engineering problems, including structural analysis. Therefore, it seems to be the most widely used software in the academic research of material and geometric nonlinear analysis due to the flexibility that it provides for the users with numerous options for materials models, analysis, and solution techniques. It is a program, based on the finite element that can solve problems ranging from relatively simple linear analyses to the most challenging nonlinear simulations. ABAQUS contains an extensive library of elements that can model any type of geometry. It has an equally extensive list of a material library that can conduct the behavior of most typical engineering materials including metals, rubber, polymers, composites, reinforced concrete, crushable and resilient foams, and geotechnical materials such as soils. ABAQUS /Standard, ABAQUS /Explicit, and ABAQUS are the three different way executions with different parameters. ABAQUS /Standard and ABAQUS /Explicit perform analysis, and ABAQUS provides a graphical environment for pre and post-processing.

ABAQUS /Standard was a general-purpose analysis program for solving linear, nonlinear, static, and dynamic problems. ABAQUS /Explicit is a special-purpose analysis program that uses an explicit dynamic finite element formulation, to sum up, the finite element program. ABAQUS is a powerful computational tool for modeling structures with material and geometric nonlinear behavior. For Creating and analyzing a model ABAQUS includes 15 modules: Part module, Property module, Assembly module, Step module, Interaction module, Load module, Mesh module, Job module, Visualization module, and Sketch module. To create a complete analysis model, it is usually necessary to go through most of these modules.

3.2. Analysis of unreinforced & reinforced masonry walls under seismic load

This study has simulated reinforced fully grouted and unreinforced fully grouted masonry walls using ABAQUS 6-16, the seismic load was taken as in cyclic loading on the exposed reinforced and unreinforced building single panel masonry wall and the simulation of this masonry walls were carried out by varying aspect ratio (H/L) and reinforcement spacing and the ratio of the walls.

3.3. Numerical Modeling of unreinforced & reinforced masonry walls

Masonry was one of the oldest and most wide-spread structural materials. It has been and is still used for various construction purposes, masonry consists of units and mortar, these constituents have their own mechanical properties and their geometry and arrangement can very forming different masonry assemblages. For numerical modeling often required understanding the structural behavior under various loading conditions.

Now day’s numerical models often a variable alternative to physical experiments. Different numerical methods such as the finite element method (FEM), discrete element method (DEM) and the applied element method (AEM) have been employed to conduct numerical analysis and simulation of linear and non-linear behavior of masonry. This paper focuses on finite element method (FEM) analysis.

The masonry wall selected for this study consists of two different types of masonry walls. Such as reinforced and unreinforced fully grouted masonry walls by applying different (H/L) aspect ratios of building walls. And this thesis paper's masonry block element model are modeled based on Paulo B. Lourenço, (2014), and K.F. Abdulla et al, (2017) state that masonry wall masonry blocks longitudinal and bad joint mortar and grouted concrete is modeled as solid element and reinforcement is modeled as a truss. To simulate seismic loading condition under quasi-static cyclic load on the exposed seismic zone constructed masonry walls (reinforced and unreinforced fully grouted) to investigate the seismic performance comparison of fully grouted reinforced and fully grouted unreinforced masonry wall building, Besides for reinforced masonry walls performance also checked because of different horizontal and vertical reinforcement ratio and spacing. The masonry wall selected for this study consists of two different types of masonry walls. Such as reinforced and unreinforced fully grouted masonry walls by applying different (H/L) aspect ratios of building walls. And this thesis paper's masonry block element model is modeled based on Paulo B. Lourenço, (2014), and K.F. Abdulla et al, (2017) state that masonry wall masonry blocks longitudinal and bad joint mortar and grouted concrete is modeled as solid element and reinforcement is modeled as a truss. To simulate seismic loading condition under quasi-static cyclic load on the exposed seismic zone constructed masonry walls (reinforced and unreinforced fully grouted) to investigate the seismic performance comparison of fully grouted reinforced and fully grouted unreinforced masonry wall building, In addition for reinforced masonry walls performance also checked because of different horizontal and vertical reinforcement ratio and spacing.

3.3.1. Element Modeling

The masonry block (HCB), masonry bed and longitudinal joint mortar and grouted concrete fill material has been modeled with eight-node hexahedral solid element C3D8R, the HCB unit is expanded by adding the mortar thickness, the expanded units are modeled as a series of continuum elements and the interaction between the expanded units is modeled as series of discontinued elements. and the horizontal and vertical wall steel reinforcement, other flexural and shear reinforcement are modeled with 3D2-noded linear truss element (T3D2) as shown in figure a, b, and c, respectively and also perfect bond or interaction considered between masonry block (HCB), bed and longitudinal joint mortar and grouted concrete is surface to surface cohesive interaction and also in reinforced masonry wall reinforcement through the embedded method in ABAQUS 6-16.

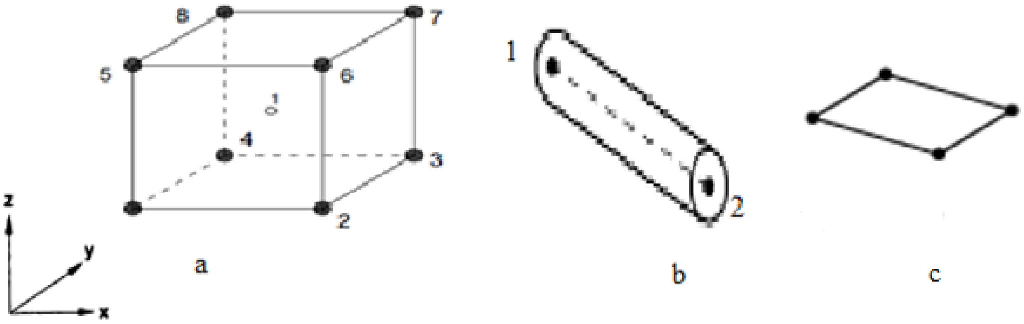

Figure 3-1 a) C3D8R hexahedral element type b) T3D2 Truss Element type c) R3D4, rigid element

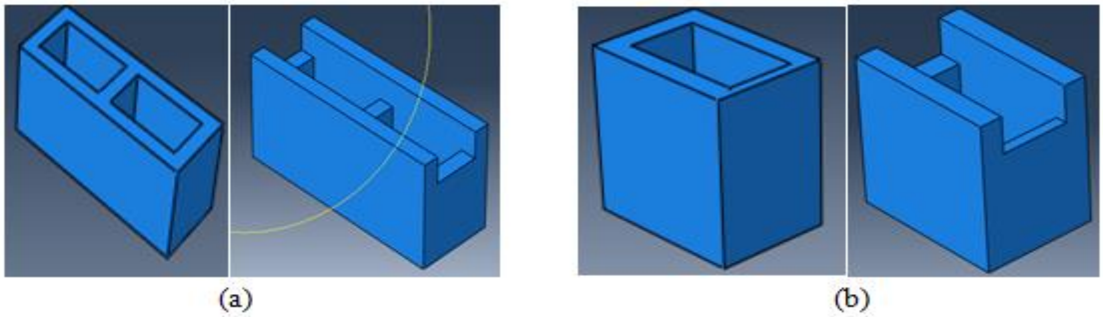

Figure 3-2 modeling of hollow concrete masonry unit (a), full HCB block model (b), half HCB block model

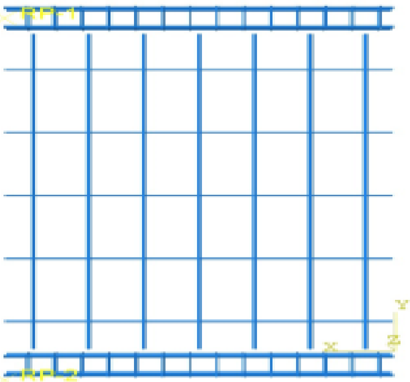

Figure 3-3 modeling of masonry wall reinforcement arrangement in masonry

3.3.2. Defining the material properties

This section specification reviews the individual behavior of masonry block (HCB), masonry longitudinal and bed joint mortar, grouted concrete fill, and steel reinforcement as they related to the strain stress relation of the material property of masonry block. Each constitutes material properties can play an essential role when undertaken and kind of non-linear finite element analysis.

3.3.2.1. Constitutive model property of fully grouted masonry wall

3.3.2.1.1. Concrete damaged plasticity model

In concrete fill and hollow concrete block of concrete damage plasticity model (CDP), users should have to enter the appropriate magnitude of various parameters. Such as, (1) parameter characterizing the performance of concrete fill and hollow concrete block under compound stress is known as dilation angle, (2) a parameter that describing the state of the material is the point in which the concrete fill and hollow concrete block undergo failure under biaxial compression which is called the ratio of the strength in the biaxial state to the strength in the uniaxial state, and (3) the plastic potential eccentricity and it is a small value which can be calculated as a ratio of tensile strength to compressive strength.

Dilation angle (ψ)

Dilation angle is the angle of inclination of the failure surface toward the hydrostatic axis, measured in the meridional plane. Physically, the dilation angle was interpreted as a concrete internal friction angle. In this thesis, the value of dilation angle used is 36^o for concrete fill and 31^o for masonry material.

Plastic potential eccentricity (ϵ)

It is a small positive value that expresses the rate of approach of the plastic potential hyperbola to its asymptote. It can be calculated as a ratio of tensile strength to compressive strength. This thesis uses both concrete fill and masonry material. The CDP model recommends assuming 0.1 values.

The ratio of the strength in the biaxial state to the strength in the uniaxial state (f_{bo}/f_{co})

ABAQUS user's manual specifies default values of f_{bo}/f_{co} as 1.16 and the same is used in this thesis for both concrete fill and masonry material.

Kc, the ratio of the second stress invariant on the tensile meridian to that on the compressive meridian at initial yield for any given value of the pressure invariant p such that the maximum principal stress is negative, $\boldsymbol{\sigma_{max}} < 0$. The default value is 2/3.

Table 3-1 Concrete fill damage plasticity model parameters

Plasticity				
Dilation angle	Eccentricity	f_{bo}/f_{co}	K	viscosity parameter
31^0	0.1	1.16	0.667	0.001

Table 3-2 Default values in CDP model of hollow concrete block as per ABAQUS user manual

Plasticity				
Dilation angle	Eccentricity	f_{bo}/f_{co}	K	viscosity parameter
15^0	0.1	1.16	0.667	0.001

3.3.2.2. Mechanical behavior grouted or concrete fills

The concrete fill and hollow concrete block model is a continuum, plasticity-based, damage model. It assumes that the main two failure mechanisms are tensile cracking and compressive crushing of the concrete material (concrete fill and hollow concrete block). The evolution of the yield (or failure) surface was controlled by two hardening variables ε_t^{in} and ε_c^{in} linked to failure mechanisms under tension and compression loading respectively. We refer to ε_t^{pl} and ε_t^{pl} as tensile and compressive equivalent plastic strains, respectively. The following sections discuss the main assumptions about the mechanical behavior of concrete.

3.3.3. Compression Stress-strain relationship of grouted or concrete fill

The stress-strain relation of concrete fill is generally defined by using the concept of concrete. The user should be entering the yield stress(σ_c), inelastic strain, ε_c^{in} corresponds to stress values and damage properties (dc) in tabular format. Therefore, total strain values should be converted to the inelastic strains using the following Eq. 3.1.

$$\varepsilon_{\boldsymbol{c}}^{\boldsymbol{in}} = \boldsymbol{\varepsilon_c} - \boldsymbol{\varepsilon_c^{el}} \quad \text{……………………………………………………… Equation 3.1}$$

Where, $\varepsilon_c^{el} = {}^{\sigma_c}/_{E_c}$ is elastic strain corresponding to the undamaged material property and ε_c is also total compressive strain. Therefore, ABAQUS after detecting the inelastic strain and damage parameter, automatically calculate the plastic compressive strain of concrete fill using the following Eq. 3.2.

$$\varepsilon_c{}^{pl} = \varepsilon_c{}^{in} - \frac{d_c}{(1-d_c)}\frac{\sigma_c}{E_c} \quad \text{.......Equation3.2}$$

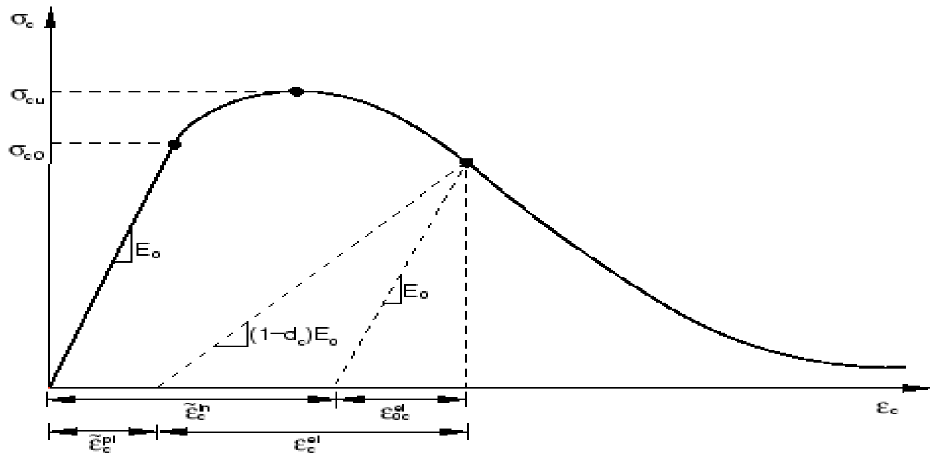

Figure 3-4 Typical compressive stress – strain relationship with damage properties (ABAQUS manual, 2016)

As shown in Figure 3.5 the unloaded response of concrete seems to be weakened because the elastic stiffness of the material appears to be damaged or degraded. The degradation of the elastic stiffness on the strain-softening branch of the stress-strain curve was characterized by damage variable dc, its range is from zero for undamaged material to one for a total loss of strength, these values can also be obtained from uniaxial compression tests, by calculating the ratio of the stress for the declining part of the curve to the compressive strength of the concrete. The compression damage variable can determine by Equation 3.3.

$$\boldsymbol{d_c = 1 - \left(\frac{\sigma_c}{E_o(\varepsilon_c - \varepsilon_c{}^{pl})}\right)} \quad \text{.......Equation 3.3}$$

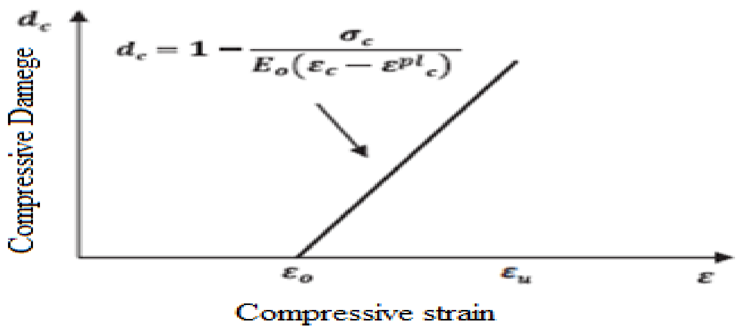

Figure 3-5 Compression Damage Property of Concrete (Wahalathantri, et al., 2011)

Generally, the stress – strain relation under uniaxial compression is taken into account by Equation 3.4 in ABAQUS.

$$\boldsymbol{\sigma_c} = (\mathbf{1} - \boldsymbol{d_c}) * \boldsymbol{E_c} * \left(\boldsymbol{\varepsilon_c} - \varepsilon_{\boldsymbol{c}}{}^{\boldsymbol{pl}}\right) \quad \text{……………..………………………Equation 3.4}$$

3.3.4. Numerical Model for Compressive Stress–Strain Relationship of Concrete fill

3.3.4.1. Stress-strain relationship for non-linear structural analysis of concrete fill

For non-linear FE analysis, a material model can play an essential role to predict the strength of concrete, ES EN 1992-1-1:2015 proposes different stress-strain relationships for concrete under uniaxial compression. For non-linear structural analysis, the relation illustrated in Figure 3.6 is recommended. The relation between σ_c and ε^c under uniaxial loading is described by Equation 3.5:

$$\frac{\sigma_c}{f_{cm}} = \frac{k\eta - \eta^2}{1 + (k-2)\eta} \qquad , is\ valid\ for\ 0 < |\varepsilon_c| < \varepsilon_{cu1}$$

Where $\eta = {}^{\varepsilon_c}/_{\varepsilon_{c1}}$, ε_{c1} is the strain at peak stress according to Table 3.1 of ES EN 1992-1-1

ε_{c1}=0.7*$(f_{cm})^{0.31}$

k=1.05$E_{cm}|\varepsilon_{c1}|/f_{cm}$

From the above equation $\sigma_c = \frac{\boldsymbol{k\eta - \eta^2}}{\mathbf{1+(k-2)\eta}} * \boldsymbol{f_{cm}}$…………………….………….. Equation 3.5

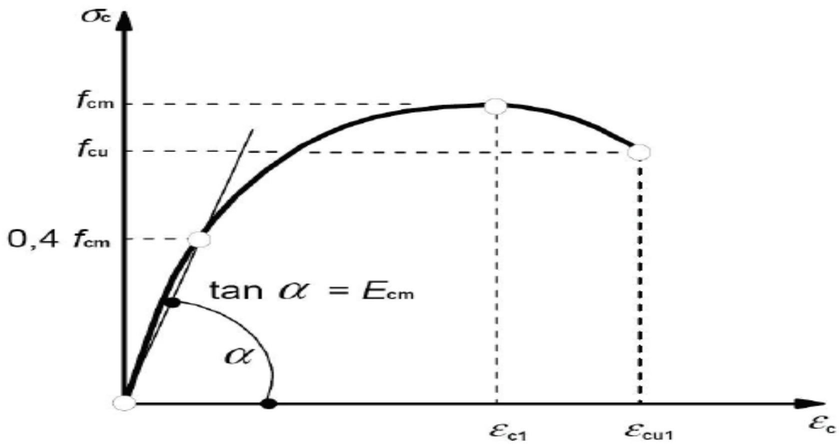

Figure 3-6 stress-strain curve for non-linear structural analysis of concrete (ES EN 1992-1-1:2015)

According to Majewski, a linear elasticity limit should increase with concrete strength and it should be rather assumed than experimentally determined and calculated as a percentage of stress to concrete strength from this formula:

$$\boldsymbol{e_{lim}} = \mathbf{1} - \boldsymbol{exp}\left(\frac{-\boldsymbol{f_c}}{\mathbf{80}}\right) \quad \text{…………………………………………..…… Equation 3.6}$$

This ceiling can be simply arbitrarily assumed as 0.4 f_{cm}. ES EN 1992-1-1 specifies the modulus of elasticity for concrete to be secant in a range of 0–0.4 f_{cm} up to linear elastic region end. Since the basic definition of the material already covers the shear modulus and the longitudinal modulus of concrete, at this stage it is good to assume such an inelastic phase threshold that the initial value of young's modulus and the secant value determined according to the standard will be convergent. In most numerical analyses it is rather not the initial behavior of the material, but the stage in which it reaches its yield strength that is investigated.

In this non-linear simulation, the material properties for masonry materials, like concrete fill, hollow concrete unit, and steel reinforcement as well as are shown in Tables 3.3 to 3.13.

The modulus of elasticity (also known as elastic modulus, the coefficient of elasticity) of concrete is a number that is defined by the ratio of the applied stress to the corresponding strain within the elastic limit or up to ε_c. Physically it indicates a material's resistance to being deformed when stress is applied to it. Modulus of elasticity also indicates the stiffness of a material. The value of elastic modulus is higher for the stiffer materials.

Modulus of elasticity of concrete fill can be defined as the slope of the line drawn from stress of zero to a compressive stress of $0.4f'_c$ and, as concrete is a heterogeneous material. The strength of concrete is dependent on the relative proportion and modulus of elasticity of the aggregate. To know the accurate value of elastic modulus of a concrete batch, a laboratory test can be done. Also, there are some empirical formulas provided by different codes to obtain the elastic modulus of concrete. These formulas are based on the relationship between modulus of elasticity and concrete compressive strength. One can easily obtain an approximate value of modulus of elasticity of concrete using 28 days concrete strength (f'_c) with these formulas. Elastic modulus of concrete from ACI code; different codes have prescribed some empirical relations to determine the modulus of elasticity of concrete. A few of them are given below, and also modulus of elasticity for concrete is calculated by using the equation below.

According to ACI 318-01 section 8.5

$E_c = \mathbf{wc^{1.5} * 0.043\sqrt{F'_C}}$ ……………………………………….………….Equation 3.7

But this formula is valid for values of w_c between 1440 and 2560 kg/m^3.

According to BN BC-2006 section 5.13.2.1

$E_c = \mathbf{44} * \mathbf{wc^{1.5}} * \sqrt{\mathbf{f'_c}}$ ....Equation 3.8

Where Wc between $15\,\frac{KN}{m^3}$ and $20\,\frac{KN}{m^3}$ and $\sqrt{f'_c}$ in MPa

Normal density concrete

$E_c = 4700 * \sqrt{\mathbf{f'_c}}$..Equation 3.9

Table 3-3 Properties Grouted Concrete Fill

Grouted Concrete fill		
Mass density (ton/mm^3)	Young's modulus (MPa)	Poisson's Ratio
2.4×10^{-9}	29000	0.2
Masonry Wall Steel reinforcement		
Mass density (ton/mm^3)	Young's modulus (MPa)	Poisson's Ratio
7.85×10^{-9}	2×10^5	0.3

Table 3-4 Compression Properties of grouting Concrete fill material

Concrete compressive strength, f'c	25
Characteristic compressive cylinder strength of concrete at 28 days, f_{ck}	25
mean value of concrete cylinder compressive strength, $f_{cm=fck+8}$	33
Secant Modulus Elasticity of Concrete, E_{cm} (MPa)	31,475.81
Compressive strain at the peak stress e_{c1}	0.0020694
Ultimate compressive Strain, e_{cu}	0.0035
e_lim	0.40
Compressive yield stress, f'_{cy} (MPa)	13.20
Compressive yield Strain, e_{cy}	0.000419

Table 3-5 Ideal stress strain relations of concrete fill material

Total Strain(e_c)	Stress σ_c (MPa)
0.0000000	0.000000
0.0004194	13.200000
0.0007494	19.916197
0.0010134	24.701137
0.0012246	27.726399
0.0013935	29.643938
0.0020694	33.000000
0.0022737	32.701858
0.0024489	31.977524
0.0025991	31.018112
0.0027278	29.950633
0.0028381	28.857794
0.0029327	27.791787
0.0035000	18.949944

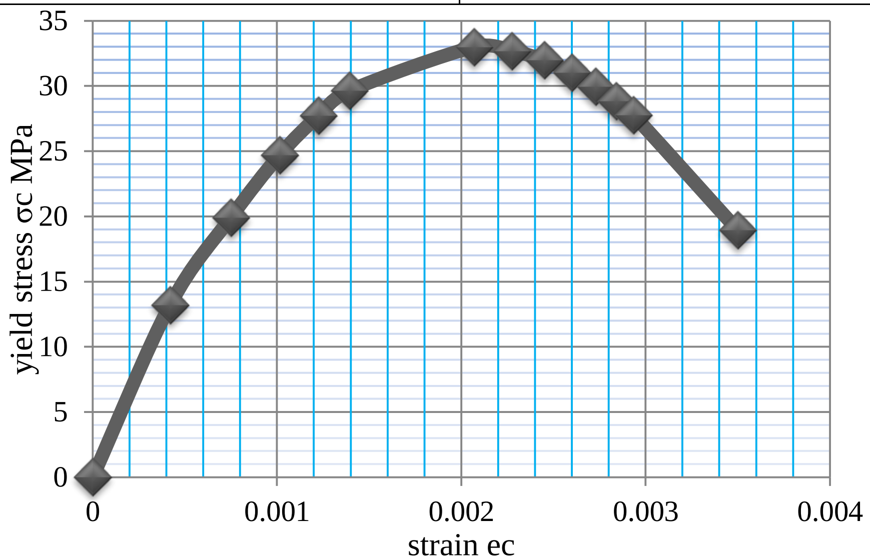

Figure 3-7 the idealized stress-strain relation of grouted concrete fill

According to Yunus Dere and Mehmet Alpaslan Koroglu (2017), the implementation of concrete damage plasticity requires the inelastic strains to describe the compressive behavior of concrete fill. The inelastic strain of concrete was obtained simply by subtracting the elastic strain from the total stain or the elastic strain corresponding to the undamaged material. Abacus will convert the inelastic strain into a plastic strain that is compatible with the masonry grouted concrete fill model.

Table 3-6 Concrete compression hardening

Inelastic Strain	Stress
0	0
0	13.2
0.000117	19.9162
0.000229	24.70114
0.000344	27.7264
0.000452	29.64394
0.001021	33
0.001235	32.70186
0.001433	31.97752
0.001614	31.01811
0.001776	29.95063
0.001921	28.85779
0.00205	27.79179
0.002898	18.94994

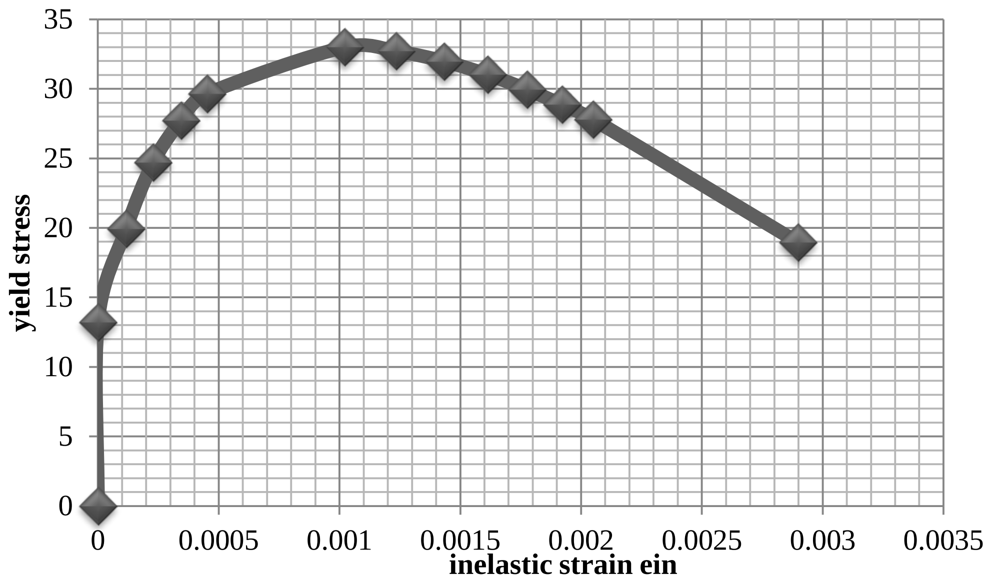

Figure 3-8 Grouted Concrete fill compression hardening

The computed plastic stain must not be negative and or decreasing with increasing inelastic strain; unless otherwise, Abacus will issue an error message as details expressed in the section.

Table 3-7 grouted Concrete fill compression damage

Inelastic Strain e_{in}	Compression damage (d_c)
0	0
0.000117	0
0.000229	0
0.000344	0
0.000452	0
0.001021	0
0.001235	0.009035
0.001433	0.030984
0.001614	0.060057
0.001776	0.092405
0.001921	0.125521
0.00205	0.157825
0.002898	0.425759

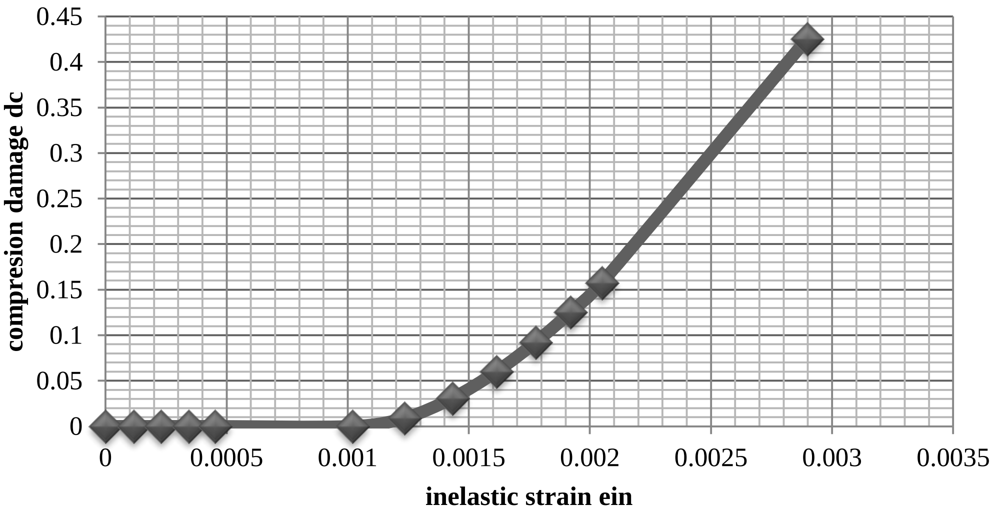

Figure 3-9 grouted Concrete fill compression damage

Tension stiffening relationship grouted concrete fill

The post-failure behavior for direct straining is modeled with tension stiffening, which allows defining the strain-softening behavior for cracked concrete along the hollow concrete block and HCB grouted concrete. This behavior also allows for the effects of the horizontal and vertical reinforcement interaction with concrete fill and HCB masonry to be simulated in a simple manner. Tension stiffening is required in the concrete damaged plasticity model for concrete fill and HCB block. Tension stiffening can be specified by means of a post-failure stress-strain relation or by applying a fracture energy cracking criterion**.**

In reinforced fully grouted wall concrete fill the specification of post-failure behavior generally means giving the post-failure stress as a function of cracking strain ε_c^{ck}. The cracking strain was defined as the total strain minus the elastic strain corresponding to the undamaged material; that is, $\varepsilon_c{}^{ck} = \varepsilon_c - \varepsilon_{ot}^{el}$, where , $\varepsilon_t^{el} = {}^{\sigma_t}/_{E_o}$, as illustrated in Figure 3.12. To avoid potential numerical problems, ABAQUS enforces a lower limit on the post-failure stress equal to one-hundredth of the initial failure stress: $\sigma_t \geq \sigma_{to}/100$.

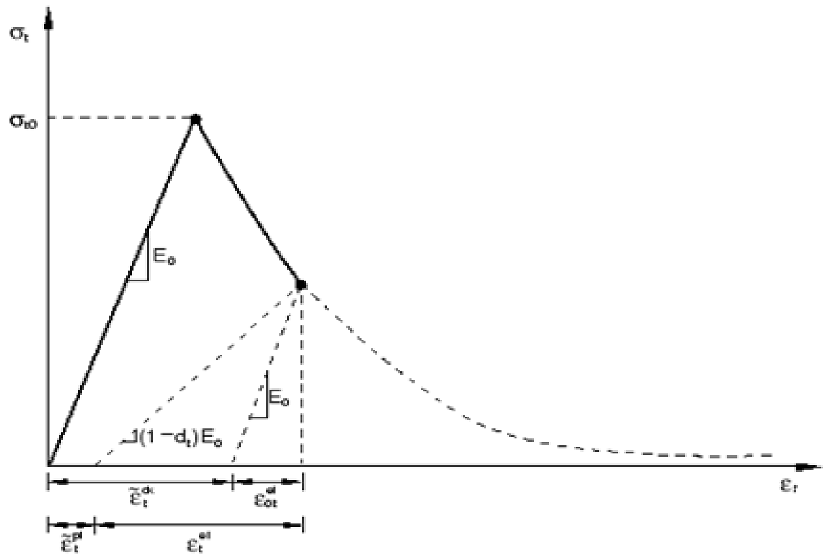

Figure 3-10 Illustration of the definition of the cracking strain used for the definition of tension stiffening data (ABAQUS manual, 2016)

Tension stiffening data are given in terms of the cracking strainε^{ck}. When unloading data are available, the data are provided to ABAQUS in terms of tensile damage curves, $d_t - \varepsilon_c{}^{ck}$, as discussed below. ABAQUS automatically converts the cracking strain values to plastic strain values using Equation 3.11.

$\boldsymbol{\varepsilon_t{}^{pl} = \varepsilon_t{}^{ck} - \frac{d_c}{(1-d_t)}\frac{\sigma_t}{E_o}}$ ……………………………..…………………..Equation 3.10

ABAQUS will issue an error message if the calculated plastic strain values are negative and/or decreasing with increasing cracking strain, which typically indicates that the tensile damage curves are incorrect. In the absence of tensile damage, $\varepsilon_t{}^{pl} = \varepsilon_t{}^{ck}$.

In cases with little or no reinforcement, the specification of a post-failure stress-strain relation introduces mesh sensitivity in the results, in the sense that the finite element predictions do not converge to a unique solution as the mesh is refined because mesh refinement leads to narrower crack bands. This problem typically occurs if cracking failure occurs only at localized regions in the structure and mesh refinement does not result in the formation of additional cracks. If cracking failure is distributed evenly (either due to the effect of rebar or due to the presence of stabilizing elastic material, as in the case of plate bending), mesh sensitivity is less of a concern.

In practical calculations for reinforced fully grouted masonry walls, the mesh is usually such that each element contains rebar. The interaction between the rebar and the masonry tends to reduce the mesh sensitivity, provided that a reasonable amount of tension stiffening is introduced in the concrete model to simulate this interaction. This requires an estimate of the tension stiffening effect, which depends on such factors as the density of reinforcement, the quality of the bond between the rebar and the masonry, the relative size of the concrete aggregate compared to the rebar diameter, and the mesh. A reasonable starting point for relatively heavily reinforced concrete modeled with a fairly detailed mesh is to assume that the strain-softening after failure reduces the stress linearly to zero at a total strain of about 10 times the strain at failure.

The choice of tension stiffening parameters is important since, generally, more tension stiffening makes it easier to obtain numerical solutions. Too little tension stiffening will cause the local cracking failure in the concrete to introduce temporarily unstable behavior in the overall response of the model. Few practical designs exhibit such behavior so that the presence of this type of response in the analysis model usually indicates that the tension stiffening is unreasonably low.

3.3.4.2. Numerical model tensile Stress – Strain relationship of concrete fill

According to Hsu and Mo., 2010, the tensile stress of concrete $\sigma_1{}^c$ is small compared with the compressive stress $\sigma_2{}^c$, but not zero. This stress $\sigma_1{}^c$ is a uniform tensile stress of concrete, representing the stiffening of the steel bars by concrete in tension. Figure 3.11 shows a typical tensile stress–strain curve of concrete. The curve consists of two distinct branches. Before cracking the stress–strain relationship is essentially linear. After cracking, however, a drastic drop of strength occurs and the descending branch of the curve becomes concave. In the descending branch, the concrete fill is cracked and the concept of concrete tensile stress $\sigma_1{}^c$ and concrete tensile strain ε_1 are quite different from those before cracking. $\sigma_1{}^c$ is defined as the smeared (or average) concrete tensile stress and $\bar{\varepsilon}_1$ is the smeared (or average) concrete tensile strain.

Based on the tests of 35 full-size panels, Belarbi and Hsu (1994) and Pang and Hsu (1995)

Proposed the following analytical expressions for the $\sigma_1{}^c - \bar{\varepsilon}_1$ curve:

Ascending branch $\breve{\varepsilon}_1 \leq \varepsilon_{cr}$

$\boldsymbol{\sigma_c^1 = E_c \overline{\varepsilon_1}}$ …………………………..……………………….. Equation 3.11

Where:

E_c =modulus of elasticity of concrete, taken as $4700\sqrt{f'c(\mathrm{MPa})}$. Where, $f'c$ and $\sqrt{f'c}$ are in MPa;

ε_{cr} =cracking strain of concrete, taken as 0.00008 mm/mm, and assume the ultimate strain=0.001

Descending branch $\varepsilon_{c1} > \varepsilon_{cr}$

$\boldsymbol{\sigma_1{}^c = f_{cr}\left(\frac{\varepsilon_{cr}}{\varepsilon_1}\right)^{0.4}}$ ……………………………………….…………….. Equation 3.12

Where, f_{cr} = cracking stress of concrete, taken as $0.31\sqrt{f'c(\mathrm{MPa})}$.

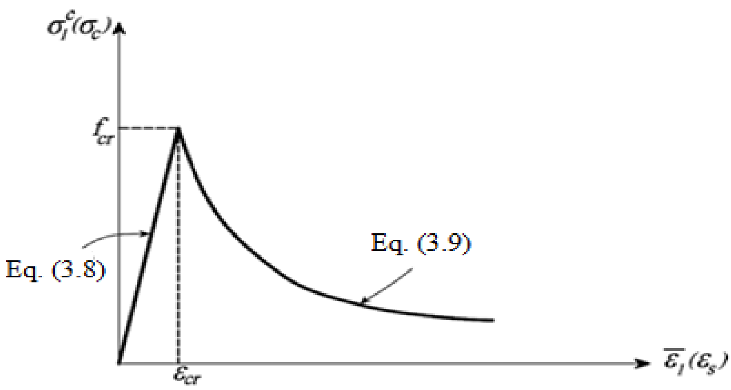

Figure 3-11 Tensile stress–strain curve of concrete (Hsu and Mo., 2010)

Table 3-8 Tension Behavior of grouted Concrete fill material

Tension behavior		
Concrete compressive strength, f'c(MPa) = 25		
Assume cracking strain of concrete = 0.00008		
Assume ultimate strain = 0.001		
Stress, MPa	Cracking Strain e_{cra}	d_t
0.000000	0.000000	0.000000
1.550000	0.000031	0.000000
0.961449	0.000233	0.379711
0.805279	0.000386	0.480465
0.728113	0.000506	0.530250
0.681908	0.000602	0.560060
0.564375	0.000982	0.635887

3.3.5. Hollow concrete block masonry (HCB) properties

It is less easy to predict the compressive strength of masonry as it depends on the properties of the masonry units, the mortar, and the grout. As a consequence, most masonry design codes specify low design values for compressive strength (f_m) unless prism tests are conducted to confirm higher values.

The compressive strength of the hollow concrete block may vary from low 1MPa for low-quality hollow concrete blocks to over 100 MPa for high-fired ceramic clay units, a minimum strength of about 1MPa is typically required by design codes (ES-EN1996, 2015), The strength of mortar test specimens bears little relationship to mortar strength in the walls. Because of the absorption of moisture from the mortar by the masonry units

Masonry properties calculate based on codes and other researcher's experimental output results, in different codes and research a sensitive calculation towards the Eu value, Attention should be paid to using a representative Eu value to avoid excessive strains, particularly considering the examples of HCB masonry. Normally, the test result showed a significant variation on Young's modulus of HCB. In his textbook (Drysdaleet al. 1994) have taken the maximum masonry compressive strain value as 0.003 based on paulay and priestley 1992. The young's modulus of masonry calculated based on Ethiopian code and standards ES-EN 1996-1-1. Design of masonry structure the equation 3.14.

$$\mathbf{E_u = 1000 * f_u} \quad \text{……………………………………………Equation 3.13}$$

Masonry unit shear modulus of rigidity may be obtained from measurements of diagonal deformations in racking test specimens. Shear modulus of masonry unit is calculated based on Ethiopian code and standards ES-EN 1996-1-1. In the absence of sufficient data, shear modulus, G_u, can be assumed to vary from 6% to 25% of the Elastic modulus (Young's modulus). The shear modulus of elasticity, G_u, was taken from the coefficient from Alcocer and Klinger (1994) in between 0.1– 0.33 times E_u (0.1 for high-strength units and 0.33 for weaker units). The shear modulus of uncracked unreinforced masonry can be estimated as G_u= 0.4 E_u in compression (FEMA 273) After cracking the shear stiffness is reduced substantially as sliding along bed joints develops or as diagonal tension cracks open. Some researchers reported that G_u value can be estimated through = 400 f'_u (Fattal and Cattaneo, 1977, Paulay and Priestley, 1992)

Table 3-9 Table HCB and mortar property

Material	f_c	f_t	E (GPa)	G (Gpa	Poission Ratio
HCB	12	1.2	6.6	2.64	0.18
M mortar	12	1.2	2.64	1.056	0.2
Grauted	25	2.5	29	11.6	0.2

The fracture energy of the unit and the mortar are computed according to Model Code 90 Thomas Ltd,s UK,1993, which are proposed for the concrete material. For values of compressive strength between 12 up to 80 MPa, the expression in equation 3.15 blow is given. On the other hand, for the tensile strength the ductility index (d_u), which is the ratio between fracture energy (G_f) and the tensile strength (f_t) ranges between 0.018 and 0.040 mm (M.Angelillo et al. 2014). The tensile strength of the HCB unit and mortar are calculated based on (M.Angelillo et al. 2014) and (G. Vasconcelos et al. 2012), its value equal to 10 percent of compressive strength. An average value for the du is taken as 0.029mm. The obtained parameters are presented in Table 3-10 below.

$$\mathbf{Gc = 15 + 0.43 * fc - 0.0036fc^2} \text{……………………………………….Equation 3.14}$$

Where: G_c = compression energy and f_c = compression strength

Table 3-10 Damage property of HCB

material	d_c	d_u	G_c (N/mm)	G_f (N/mm)
HCB	0.8	0.029	19.64	0.0348
Mortal	1.3	0.029	19.64	0.0348

$G_f = d_u * f_t$

Where: G_f = fracture energy

d_u = tensile strength ductility index

f_t = tensile strength

3.3.6. Constitutive model of wall reinforcing bar steel

In ABAQUS reinforcement in concrete structures is typically provided through Rebar's, which are one-dimensional rods that can be defined singly or embedded in oriented surfaces. Rebar's are typically used with metal plasticity models to describe the behavior of the rebar material and are superposed on a mesh of standard element types used to model the masonry.

With this modeling approach, the concrete behavior is considered independently of the rebar. Effects associated with the rebar/concrete fill and HCB block interfaces, such as bond-slip and dowel action, are modeled approximately by introducing some "tension stiffening" into the concrete modeling to simulate load transfer across cracks through the rebar. Details regarding tension stiffening are provided below.

Defining the rebar can be tedious in complex problems, but this must be done accurately since it may cause analysis to fail due to lack of reinforcement in key regions of a model. The strength and deformation properties are commonly defined from the parameters in Table 3.11.

Table 3-11 Common reinforcing steel parameters

Parameter	Description
F_{yk}	Characteristic yield strength
F_{tk}	Characteristic tensile strength
$(f_t/f_y)k$	Characteristic ratio of tensile strength to yield strength
ε_{suk}	Characteristic ultimate strain
E_{cm}	Mean values of modulus of elasticity

The ductility, which is the ability of the steel to undergo large deformation under tensile force, is of special interest with regard to plastic deformation capacity. The ductility class is defined according to the ultimate strain and the ratio of tensile strength to yield strength. The reinforcement shall have adequate ductility as defined by the ratio of tensile strength to the yield strength, $(f_t/f_y)_{k,}$ and the elongation at maximum force, ε_{uk}.

Depending on the production method, reinforcing steel is commonly classified into two categories: hot-rolled steel and cold-worked steel. The difference can easily be recognized by the shape of the stress-strain diagram for each type, as illustrated in Figure 2.4. Hot-rolled steel usually exhibits evident yield stress, followed by a plastic plateau, and subsequently by an increase in stress due to the strain hardening effect. The ratio of tensile strength to yield strength and the ultimate strain are usually high.

The characteristic yield stress f_{yk} corresponds to the lower 5% fractile of the upper yield stress. On the other hand, it is not possible to clearly identify the yield stress for cold-worked steel from the stress-strain diagram. Instead, a value of stress, called proof stress and corresponding to the stress that produces a remaining strain of 0.2%, is normally used in the design. The characteristic proof stress $f_{0.2k}$ corresponds to the lower 5% fractile of the proof stress. The strain hardening and plastic deformation capacity of cold-worked steel are relatively small, and no plastic plateau can be distinguished in the stress-strain diagram. The stress-strain curve for typical hot rolled and cold-worked steel is shown in Figure 3.12 (a) and (b).

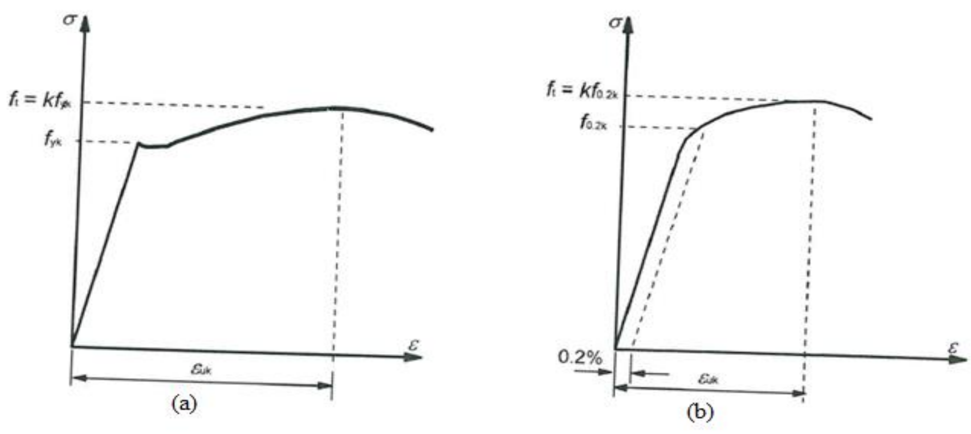

Figure 3-12 Idealized & design stress-strain diagrams for reinforcing steel for tension & compression (ES EN 1992-1-1:2015)

The value of k= $(f_t/f_y)_k$ and ε_{uk} for class A,B and C are given in Annex C of ES EN (1992-1-1:2015), Therefore, the material properties and stress-strain relation of steel reinforcement as shown in Table 3.12 to 3.13 was adopted based on the above expression of steel reinforcement parameters, stress- strain curve of hot rolled steel and using modulus of elasticity of $2x10^5$ MPa and ductility class-B.

Table 3-12 Material properties of steel reinforcement

Properties	Vertical steel reinforcement of walls	Horizontal steel reinforcement of walls
Yield strength, f_y(MPa)	420	420
Strain at yield, ε_{sy}	0.002142857	0.002142857
Tensile strength, f_{tk}(MPa)	504	504
Characteristic strain at max. force, ε_{uk}	0.02	0.02

Table 3-13 Plastic properties of horizontal & vertical steel reinforcement of masonry walls

Vertical & horizontal steel reinforcement of walls		
Stress	Strain	plastic strain
0	0	0
420	0.002143	0
436.8	0.005714	0.009489
450.24	0.008571	0.01708
460.992	0.010857	0.023153
469.5936	0.012686	0.028011
504	0.02	0.047444

3.4. Interaction properties between elements

The individual modeled elements should be connected properly to each other after assembling the structural and non-structural elements. In any type of finite element analysis, to contact and create a proper interaction between the elements is an essential part. Thus in the current investigation of finite element analysis, when two solid elements touch, contact stress might be transmitted across their common surface, and therefore determining these areas and the stress transmitted is imperative.

The full constrained contact behavior in ABAQUS is defined using tie constraints. So, the tie contact technique was utilized to create proper interaction between two elements to avoid the shear interaction. Defining the master and slave surfaces of the modeled element is necessary to create proper interaction between two elements. Defining the master and slave surfaces is a significant process when it comes to generating mesh in the sections because it leads to contact completely to the nodes on both surfaces.

A full bond between the reinforcement bars and masonry walls was achieved by modeling the reinforcement as embedded in the masonry wall concrete. Thus, the embedded technique was used to constraint the two-node truss elements (steel reinforcement) into the solid element (masonry block masonry mortar and grouted concrete fill) to create a proper bond action.

Automatic surface-to-surface contact algorithms were utilized to model the interactions between the masonry bock, longitudinal joint mortar, bed joint mortar, and grouted concrete fill. From this interaction, it is possible to develop a seismic response due to cyclic displacement that can be used to compare results with experimental values and results published by other researchers.

Penalty constraint formulation is used for contact constraint enforcement. The main advantage of using the penalty technique is to provide a realistic stiffness behavior into the model that can influence the stable time increments. Contact was modeled between concrete fill masonry block, masonry mortar, and grouted concrete. The contact in the normal direction was modeled as “Hard Contact” and in the tangential direction was modeled with a friction coefficient of 0.5, also uses cohesive constraint between mortars, hollow concrete block, and grouted concrete fill,

To make block and mortar interact to gather in a model, it was necessary to define the relationship between them. The interactions module of ABAQUS was used to do this. The contact between the surfaces was established through the option called surface to surface contact, where three contact properties were defined. Like hard contact, tangential and cohesive behavior, detail is shown in the table below.

I. Hard contact

Has the ability to prevent surface penetrates other surface and also allows a separation between them, after the contact is established.

II. The tangential behavior

Contact can reproduce the friction that occurs on the connection between the materials. It is defined by the static friction coefficient (ψ). It obeys the Columb low, in which the shear strength increases due to the increase of the compression stress. Two features in this contact must be taken into consideration. The first one is the part of the cohesion that is despised, and the second one is the possibility of establishing a critical shear stress max. When the shear stress reaches this critical value, the slipping between the surfaces will occur without an increase in shear strength, regardless of the magnitude of the compressive stress.

III. Cohesive behavior

The linear elastic properties of the surface which include the stiffness components in the traction-separation stiffness matrix are computed according to equations 3.16 and 3.17 based on (K F Abdulla et al. 2017). The cohesive behavior of the interface between the HCB unit and mortar is the works like a zero thickness bind, for which you can specify the normal stiffness K_{nn} and tangential stiffness K_{ss}, K_{tt} of the interface. The components of stiffness K_{nn} K_{ss} and K_{tt}, for joint interfaces in a simplified masonry Micro-model (interfaces between expanded masonry units), should be equivalent to the stiffness of the original masonry joint interfaces (HCB unit and mortar) under the same boundary conditions. So, the equivalent stiffness for joint interfaces is expressed as a function of the mortar's and unit's moduli of elasticity, and the thickness of the mortar Equations below based on K F Abdulla et al. (2017). The mortar thickness is assumed to be 10mm and the elastic properties of constituents are given in table 3.10. This cohesive interface property calculated stiffness parameter as shown in the table below.

$K_{nn}=\frac{E_u * E_m}{h_m(E_u - E_m)}$ ……………………………………………………….Equation 3.15

$K_{nn}=\frac{(6600N/mm2*2640N/mm2)}{10mm(6600N/mm2-2640N/mm2)} = 440\ N/mm^3$

$K_{ss} = K_{tt} = \frac{G_u * G_m}{h_m(G_u - G_m)}$……………………………………………………..Equation 3.16

$K_{ss} = K_{tt} = \frac{(2640N/mm2*1056N/mm2)}{10mm(2640N/mm2-1056N/mm2)} = 176\ N/mm^3$

Where, E_u and E_m elastic modulus of HCB unit and mortar joint respectively

G_u and G_m Shear modulus of HCB unit and mortar joint respectively

K_{nn} and K_{tt} Normal stiffness and tangential stiffness of interface respectively

Table 3-14 Cohesive behavior interface property of studied walls

Normal Direction K_{nn} (N/mm^3)	Shear I Direction K_{ss} (N/mm^3)	Shear II Direction K_{tt} (N/mm^3)
440	176	176

The damage initiation for this paper was formulated to conform to the quadratic stress criterion which is defined from the contact stresses in the interface. The normal contact for this criterion is defined from the tensile strength of the bond according to P.B.Lourenco et al. 1996. Range from 0.3 up to 0.9MPa, the model I fracture energy responds to this normal behavior ranges from 0.005 up to 0.02N/mm. The shear tractions are related to the cohesive parameter(c) for zero confined stress or also known as the initial shear strength. Values for the shear tractions range from 0.1 up to 1.8MPa and the mode II and III fracture energy thereafter ranges from 0.01up to 0.25N/mm. Since the mortar is a high strength, upper bound values are used for this paper and shown in Table 3-15 below. For the damage evaluation a Benzeggagh-Kenane (BK) formulation, which is energy-based and has a linear softening

Table 3-15 Damage parameters for the cohesive (P.B.Lourence et al.,1996)

Damage initiation			Damage evaluation		
t_n^{max} N/mm^2	t_s^{max} N/mm^2	t_i^{max} N/mm^2	G_F^I N/mm	G_F^{II} N/mm	G_F^{III} N/mm
0.8	1.0	1.0	0.02	0.2	0.2

Sensitive analysis performs K. F. Abdulla et al. 2017. Show that the viscosity parameter of 0.002 provides a stable analysis and avoid convergence problem.

Table 3-16 Cohesive Behavior Interface Property of Validation Walls

Normal Direction K_{nn} (N/mm^3)	Shear I Direction K_{ss} (N/mm^3)	Shear II Direction K_{tt} (N/mm^3)
448.6078431	179.4431373	179.4431373

Source: K F Abdulla et al. 2017and Abaqus manual 2016

This kind of contact causes a stiffness degradation called damage, in which it is only necessary to provide the interface's fracture energy. The input parameters to define the interface properties are presented in Table 3-14, 3-15, and 3-16. Damage interface property of walls was calculated based on K F Abdulla et al. 2017.

3.4.1. Boundary conditions

Constraints were applied to constrain nodal rotation and displacement in X, Y, and Z directions on the nodes located on the bottom side of masonry walls.

3.4.2. Initial conditions and Loads

Masonry walls are initially subjected to uniform gravity load in the y-direction. Also, uniform axial stress is applied on the top of the wall because of the top-loading beam in the y-direction and lateral cyclic displacement also applied on the top of the wall in the direction of x-direction. This cyclic displacement magnitude depends on the amplitude. The amplitude of lateral displacement has presented in Figure 4.4 in chapter 4

4. FINITE ELEMENT ANALYSIS RESULTS AND DISCUSSION

4.1. Introduction

In this work, the result obtained from validation and parametric studies were discussed, including accuracy of FEM analysis of masonry wall subjected by the seismic load, from validation of the ABAQUS program, the hysteresis, stiffness degradation, and displacement Ductility of the wall was displayed.

4.2. Finite element model and validation

To assess the validity of the finite element model simulation result to the experimental test simulation result. Validation of finite element analysis has done used to check the accuracy of the Finite element analysis results with experimental test results. So the goal of the comparison of finite element model simulation and experimental study was to ensure that the element material properties and convergence criteria are adequate to the model response of members and make sure that simulation processes of finite elements exactly represent the experimental work simulation.

The mechanical model of this thesis validated by comparison with numerical and experimental results available in the literature tests on shear walls was carried by Seif ElDin H. M and Galal K (2018), used to validate the numerical analysis. In the reinforced masonry wall model both numerical and experimental simulation results match the ultimate load resistance and stiffness degradation result. The finite element models were created units force (N), dimensions (mm), and time (second).

4.2.1. Experimental reinforced masonry walls parameter

M. Hany self ElDin, and Khaled Galal (2016) study the effects of horizontal reinforcement anchorage end detail of reinforced masonry shear walls subjected by the seismic load. In this study, the cross-section dimension of masonry shear wall 1600mm length, 1800mm height, and 200mm thickness. And the bottom beam cross-sectional dimension is 450mm depth, 640mm width, and 2300mm length.

4.2.2. Material property and details

The experimental model of reinforced HCB fully grouted masonry wall lies reinforcement along the horizontal and vertical direction. Wall reinforcement dimensions and property are given based on Canadian code horizontal reinforcement dimension 10M@c/c400mm center to center spacing also the vertical reinforcement dimension and spacing 20M@c/c200mm center to center.

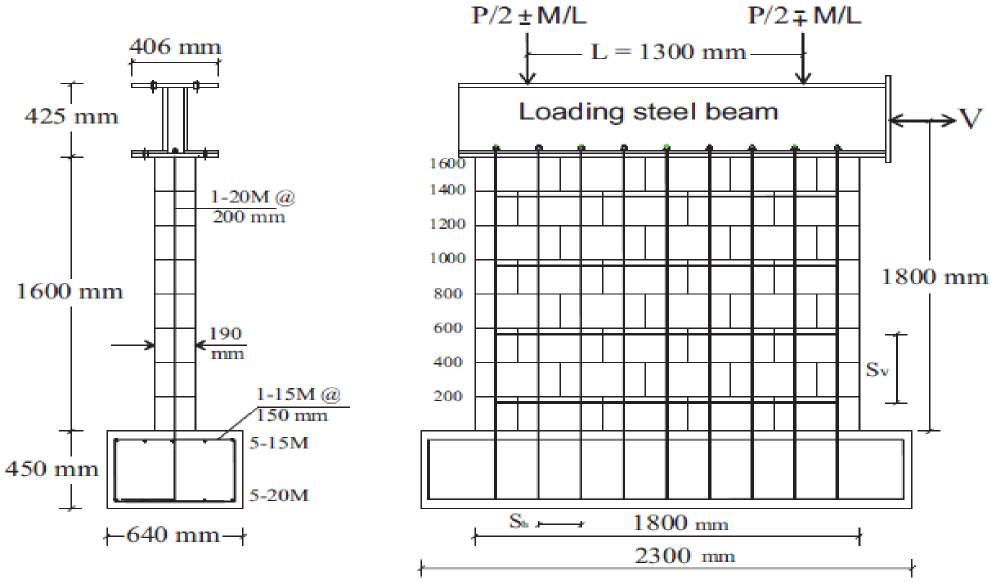

Figure 4-1 experimental reinforced masonry wall geometry and setup

4.2.3. Experimental Hollow block, mortar, concrete grout & reinforcement properties

Seif ElDin H. M and Galal K (2018) work experimental research based on this research the material properties of reinforced masonry wall the compressive strength of hollow masonry block, mortar, and grouted concrete are 13.7MPa, 16.7MPa, and 29.4MPa respectively. And also for walls and bottom beam reinforcement steel yield strength is 430MPa.

4.2.4. Geometry

The reinforced masonry wall specimens have cross-sectional dimensions of 1600 mm in height, 200 mm in width, and 1800 mm in length. And also the bottom beam dimension 450mm in depth, 640 mm width, and 2300 mm in length. The finite element model of the reinforced masonry wall test setup was presented as shown in Figure 4-2 to Figure 4-6. A three-dimensional model has been used to model the HCB block, grouted concrete fill, and mortar using the Langrangian formulation. The masonry block (HCB), masonry bed joint mortar, longitudinal joint mortar, and grouted concrete fill material have been modeled with eight-node hexahedral solid element C3D8R. And the horizontal and vertical wall steel reinforcement is modeled with a 3D 2noded linear truss element (T3D2). Interaction between masonry block (HCB), bed and longitudinal joint mortar, and grouted concrete is surface to surface cohesive interaction, and in reinforced masonry wall and reinforcement through the embedded method in ABAQUS 6.16.

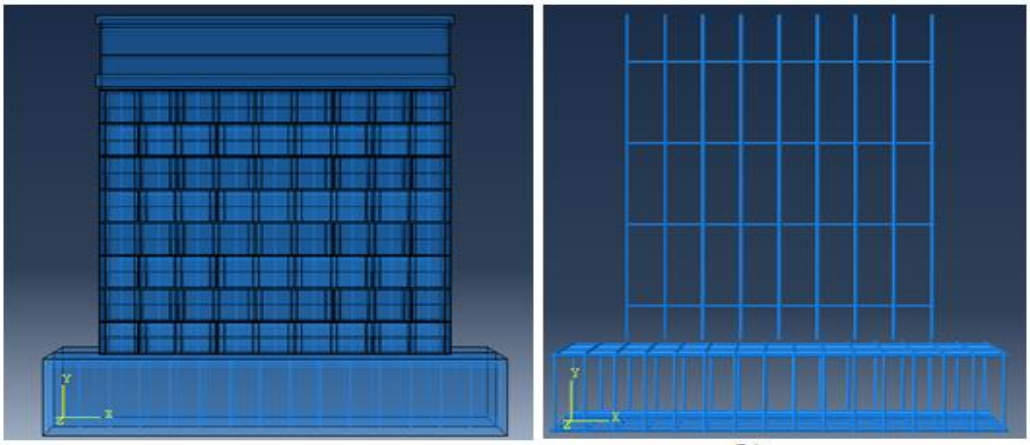

(a) (b)

Figure 4-2 (a) FEM of masonry & steel, (b) FEM of wall steel reinforcement

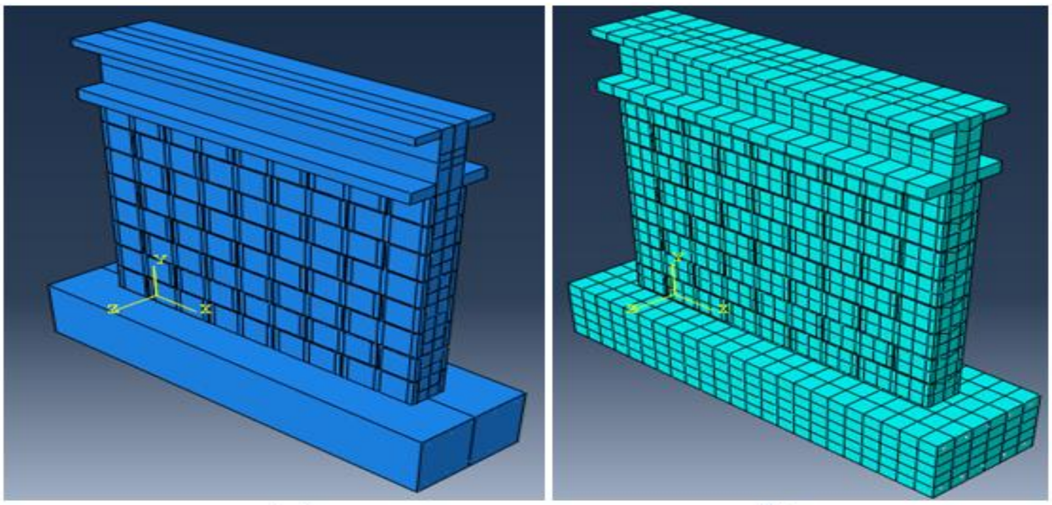

(a) (b)

Figure 4-3 (a) FEM of Reinforced masonry (RM) wall, (b) Discretized FEM of RM wall

4.2.5. Loading and cyclic load test protocol

According to Seif ElDin H. M and Galal K (2018), the load is applied to the walls in two phases. 1st phase vertical compression axial stress induced on the wall at the top end because of the top steel beam in the downward direction, next to the test protocol switched (first compression phase ended) to displacement control. In this second phase in the plane, lateral cyclic displacement was induced at the mid-height of the top steel beam, the loading protocol was proposed by FEMA 461(2007).

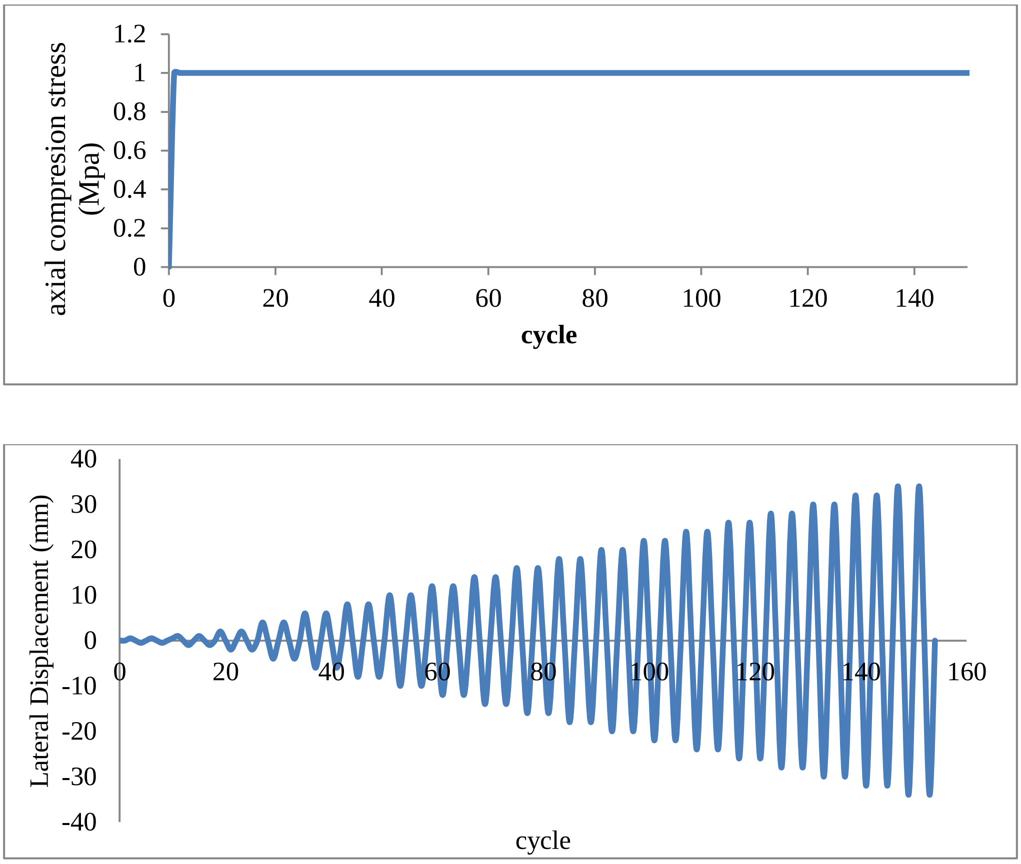

Figure 4-4 Loading procedure base on FEMA 461(2007)

4.2.6. Boundary Conditions

The reinforced masonry wall was supported at the bottom by the reinforced concrete rigid beam. This bottom beam does not rotate and is not displaced; these indicate all directional movement rotation and displacement are restraint.

4.2.7. Validation RM wall finite element result

The experiment result reported by Seif ElDin H. M and Galal K (2018), were compared with the hysteretic force-displacement response from analysis because of two loading phases of reinforced masonry shear wall based on FEMA 461(2007) cyclic load protocol show figure 4.4 above. The reinforced masonry wall experimental and numerical envelops hysteretic results are shown in Figures 4-5 and 4.6 below. The average error of numerical results for ultimate pick lateral load and lateral displacement of a reinforced masonry wall at the top end of the wall is 2.31% and 19.11%, respectively. But the displacement error numerical was high. Because in the experiment the wall vertical reinforcement highly stiff, or in an experiment, vertical Reinforcement was joined to the top steel beam by a bolt. Overall the lateral pick ultimate load and lateral displacement at the top of the reinforced masonry wall were in good agreement with the experimental analysis result.

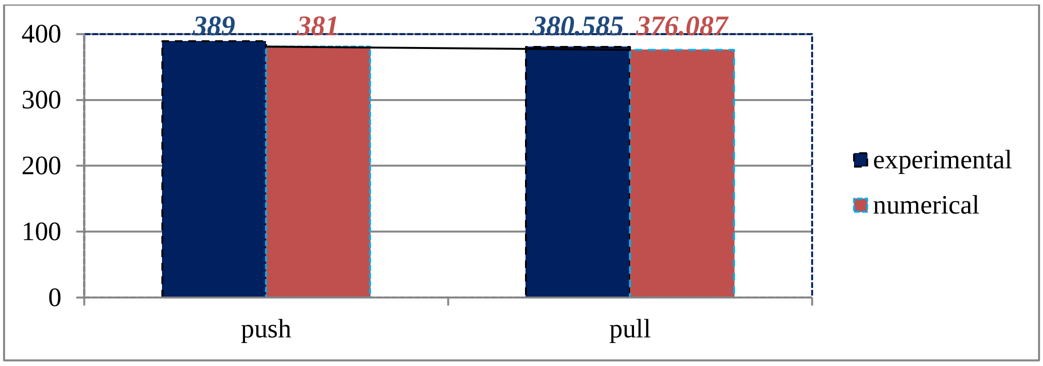

Figure 4-5 Comparison of ultimate pick lateral load of experimental and numerical result

From finite element analysis, also the cracking pattern of the wall was in good agreement with the experimental cracking pattern lines or failures. Show Figure 4-8 below

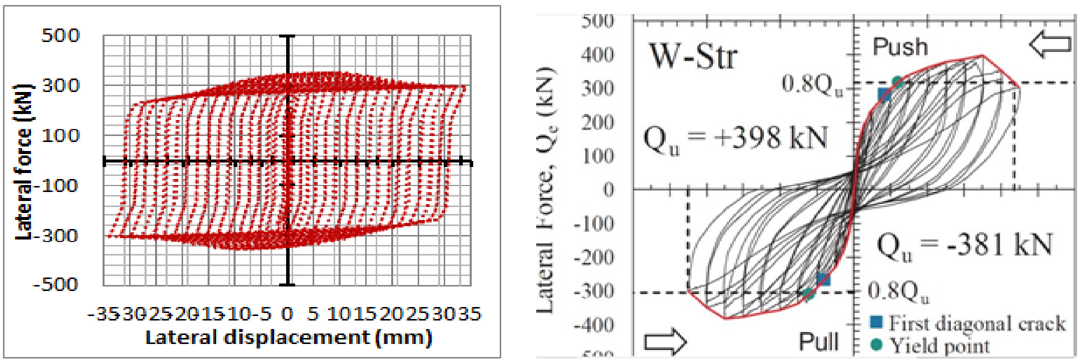

a) b)

Figure 4-6 Hysteresis curve of RM a) numerical and b) experimental

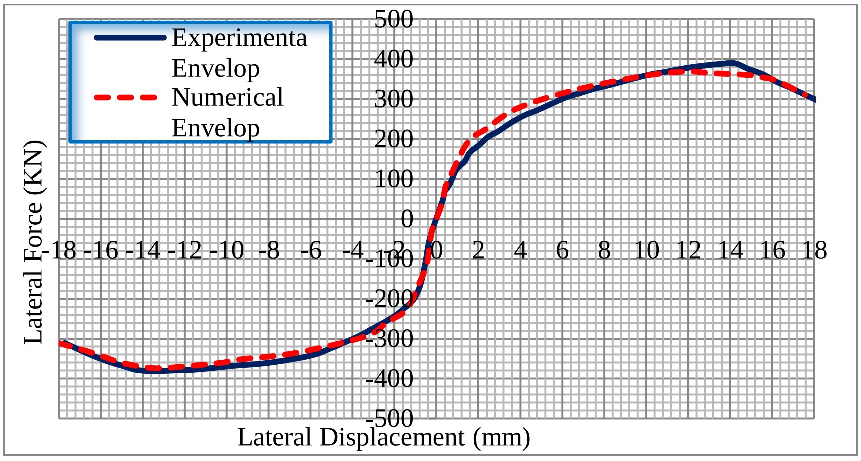

Figure 4-7 Numerical and Experimental hysteresis envelopes for wall

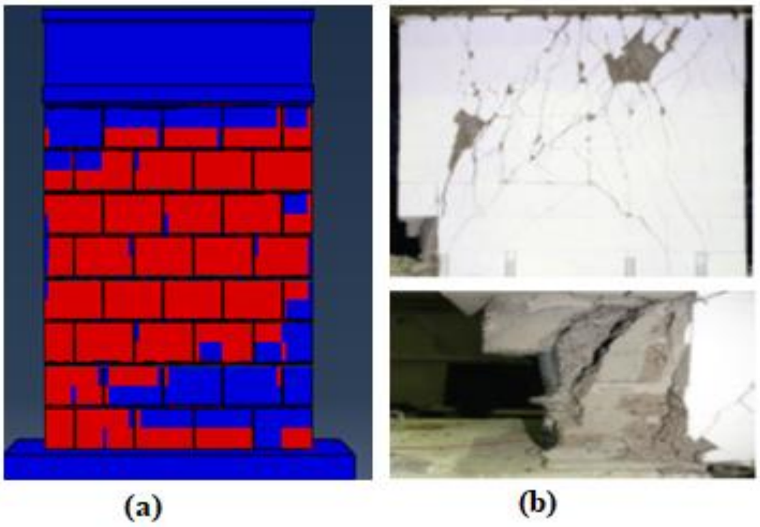

Figure 4-8 (a) Numerical cracking pattern, (b) experimental cracking pattern

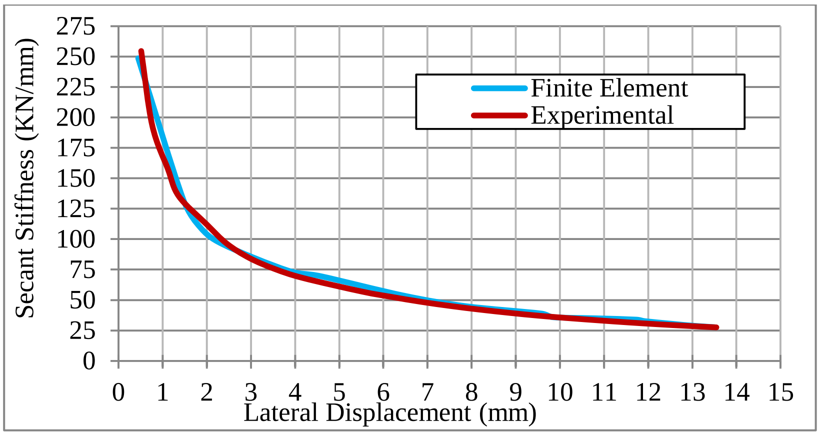

Figure 4-9 Secant stiffness degradation of the experimental and numerical output result

In above Figure 4-9, the initial secant stiffness of reinforced masonry wall experimental and finite element result was 259kN/mm and 248kN/mm respectively, the percentage error of this finite-element result is 4.435%. This result shows the finite-element results are valid in this research.

4.3. Masonry type parametric study of seismic performance

This chapter presents hysteretic behavior, stiffness degradation, and displacement ductility capacity of the reference reinforced fully grouted masonry wall and unreinforced fully grouted masonry wall by different aspect ratio (H/L) obtained through non-linear analysis. For detail recognizing the seismic performance of reinforced and unreinforced fully grouted masonry walls, the following different parameters are used. Those parameters were checking the performance of masonry wall under seismic load by changing aspect (H/L) ratio, reinforced use on the wall, spacing of horizontal reinforcement, spacing of vertical reinforcement, reinforcement ratio of horizontal reinforcement, and reinforcement ratio of vertical reinforcement. The modeled masonry wall parameter show in table 4-1 to 4-3 below

Investigate the effect under seismic load on selection masonry type was performed with the same material and geometrical properties. Compare the effect of the seismic load in masonry walls based on carrying capacity, stiffness degradation, and Ductility

Table 4-1 Studied Masonry wall parameter detail

Masonry id	representation	length	height	Aspect ratio
Wall 1	W1	1435mm	2000mm	1.39
Wall 2	W2	1435mm	2800mm	1.95
Wall 3	W3	1435mm	3200mm	2.23

Table 4-2 Unreinforced fully grouted wall matrix

wall ID	Height (mm)	Length (mm)	aspect ratio (H/L)	Reinforcement		Grouted Type
				vertical	horizontal	
W1B	2000	1435	1.39	No	No	Fully
W2B	2800	1435	1.95	No	No	Fully
W3B	3200	1435	2.23	No	No	Fully

Table 4-3 Reinforced fully grouted masonry wall matrix

Wall ID	aspect ratio (H/L)	Vertical Reinforcement			Horizontal Reinforcement		
		Φ (mm)	Reinforcement Ratio (%)	Spacing (mm)	Φ (mm)	Reinforcement Ratio	Spacing (mm)
W1C	1.39	16mm	0.65%	200mm	10mm	0.13%	400mm
W1D	1.39	16mm	0.37%	400mm	10mm	0.13%	400mm
W1E	1.39	16mm	0.65%	200mm	10mm	0.26%	200mm
W2C	1.95	16mm	0.65%	200mm	10mm	0.13%	400mm
W2D	1.95	16mm	0.37%	400mm	10mm	0.13%	400mm
W2E	1.95	16mm	0.65.%	200mm	10mm	0.26%	200mm
W3C	2.23	16mm	0.65%	200mm	10mm	0.13%	400mm
W3D	2.23	16mm	0.37%	400mm	10mm	0.13%	400mm
W3E	1.95	16mm	0.65%	200mm	10mm	0.26%	400mm

4.3.1. Aspect ratio (H/L) variation on reinforced masonry strength

The effect of aspect ratio (H/L) on the seismic performance of masonry walls was studied. The effect of aspect ratio on seismic performance of masonry walls was investigated using three walls with different aspect ratios (1.39, 1.95, and 2.23) but similar vertical and horizontal spacing. The seismic performance of the walls was expressed in terms of stiffness degradation, carrying capacity, and ductility. The study masonry walls parameters are displayed in Table 4-4 below,

Table 4-4 matrix of studied wall in the different aspect ratio

wall ID	aspect ratio (H/L))	Reinforcement dimension		Reinforcement spacing		Grouted Type
		Vertical	horizontal	vertical	horizontal	
W1C	1.39	Ø16mm	Ø10mm	200mm	400mm	Fully
W2C	1.95	Ø16mm	Ø10mm	200mm	400mm	Fully
W3C	2.23	Ø16mm	Ø10mm	200mm	400mm	Fully

The numerical results of the numerical analysis of three types of masonry of walls display, in Table 4-5. An increase in the wall aspect ratio (H/L) (from 1.39 to 2.23) shows a significant influence on the shear strength of the masonry walls for the same reinforcement distribution and axial compression stress on the wall.

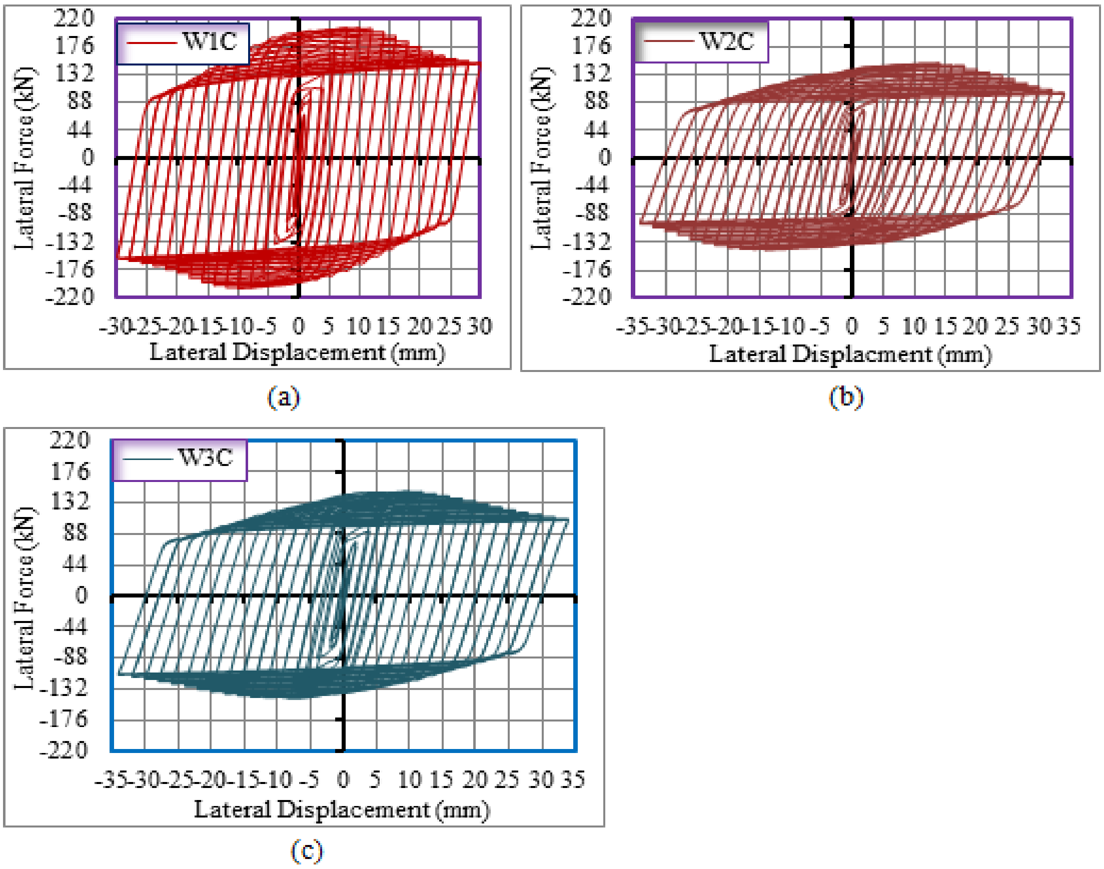

Figure 4-10 Hysteresis curve of reinforced masonry wall: (a) W1C, (b) W2C, and (c) W3C

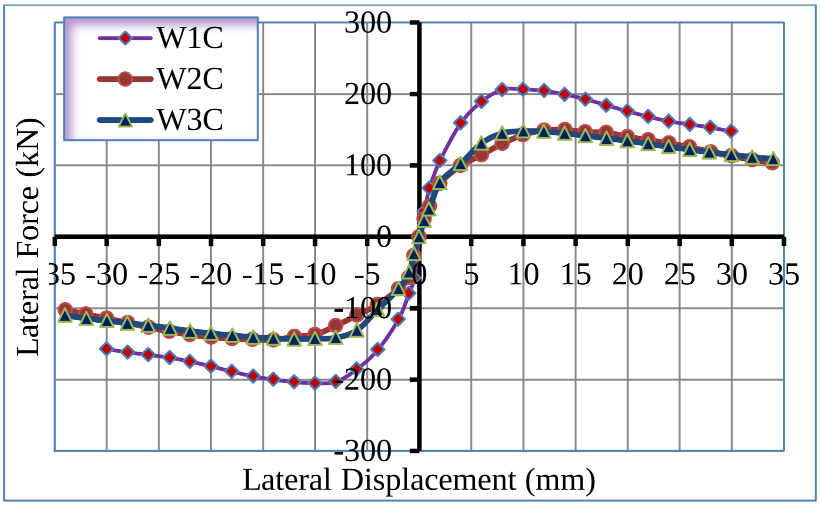

Figure 4-11 Comparison of hysteresis envelop curve of RMW with the different aspect ratio

The above figure 4-11 shows that both vertical and horizontal reinforcement ratios of the reinforced masonry models are the same but increasing the aspect ratio from 1.39 to 2.23 causes a decrease in the lateral load resistance of reinforced masonry walls

Table 4-5 Ultimate shear resistance of RMW with horizontal reinforcement ratio 0.13% but the different aspect ratio

Wall ID	Aspect (H/L) ratio	PU			
		Push (kN)	Amplification %	Pull (kN)	Amplification %
W1C	1.39	206.921	----	-205.151	----
W2C	1.95	149.776	-38.154	-144.587	-41.888
W3C	1.23	147.917	-39.890	-143.236	-43.226

From above Table 4.5 for W1C, the ultimate shear resistances for push and pull directions are 206.921kN and 205.151kN, respectively, and for W2C for Push and pull directions are 149.776kN and 144.587kN, respectively. This result shows that an increase in aspect ratio from 1.39 to 1.95 resulted in the decrease in the shear resistance by 38.15% for push direction and 41.89% for pull direction, respectively.

The result shows that the increase in aspect ratio (H/L) from 1.39 to 2.23 has a significant influence on the lateral load resistance and displacement ductility of the masonry wall, this mainly refers to the fact that by increasing the (H/L) ratio the wall failure mechanism approaches to flexural failure mechanism before reaching the shear capacity of the wall.

Displacement ductility

From the analysis of every earthquake which happened the structure has high storage for a higher earthquake than its basic earthquake, Structures use ductility to resist the seismic load. The displacement ductility is generally used as a measure of inelastic deformation capability of the structure subjected to seismic loads and can be defined as equation 4.1.

$\mu = \frac{\boldsymbol{\delta u}}{\boldsymbol{\delta y}}$ …………………………………………………………..……..Equation 4.1

Table 4-6 Displacement ductility comparison of RMW with different aspect (H/L) ratio

Wall ID	Δ_y (mm)		Δ_u (mm)		$\mu = \frac{\delta u}{\delta y}$		Amplification%	
	push	pull	push	pull	push	pull	Push	pull
W1C	4.824	4.891	9.974	10.0	2.068	2.044	---	----
W2C	5.521	5.468	13.328	13.359	2.414	2.443	16.73%	19.52%
W3C	5.722	5.671	13.975	13.9834	2.442	2.466	18.08%	20.64%

For the wall with an aspect ratio of 1.95 the displacement ductility of W2C for push and pull directions are higher than that of W1C by 16.73% and 19.52% respectively. And the displacement ductility of W3C for push and pull directions are higher than that of W1C by 18.08% and 20.64% respectively. This result indicates that the aspect ratio affects the displacement ductility of masonry walls. The wall failure modes of all walls are flexure failure shown in figure 4.12 below.

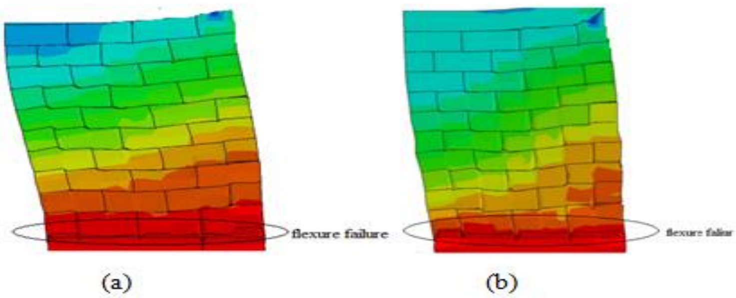

Figure 4-12 Detailing Failure of masonry wall (a), W1D (b), W1I

4.3.2. Effect of reinforcement used in a wall on seismic performance of wall failure

In this portion, the seismic performance of fully grouted unreinforced masonry walls and fully grouted reinforced masonry walls are investigated. Additionally, a comparison is made on the seismic resistance of those walls. To see the effect of using reinforcement on the performance of walls, the aspect (H/L=1.95) ratio of the walls, the materials used, and load magnitude are kept the same.

Table 4-7 Matrix of the studied wall with reinforced and unreinforced fully grouted masonry

wall ID	aspect ratio (H/L)	Reinforcement dimension		Reinforcement spacing		Grouted Type
		vertical	horizontal	vertical	Horizontal	
W2B	1.95	---	---	---	---	Fully
W2C	1.95	Ø16mm	Ø10mm	200mm	400mm	Fully

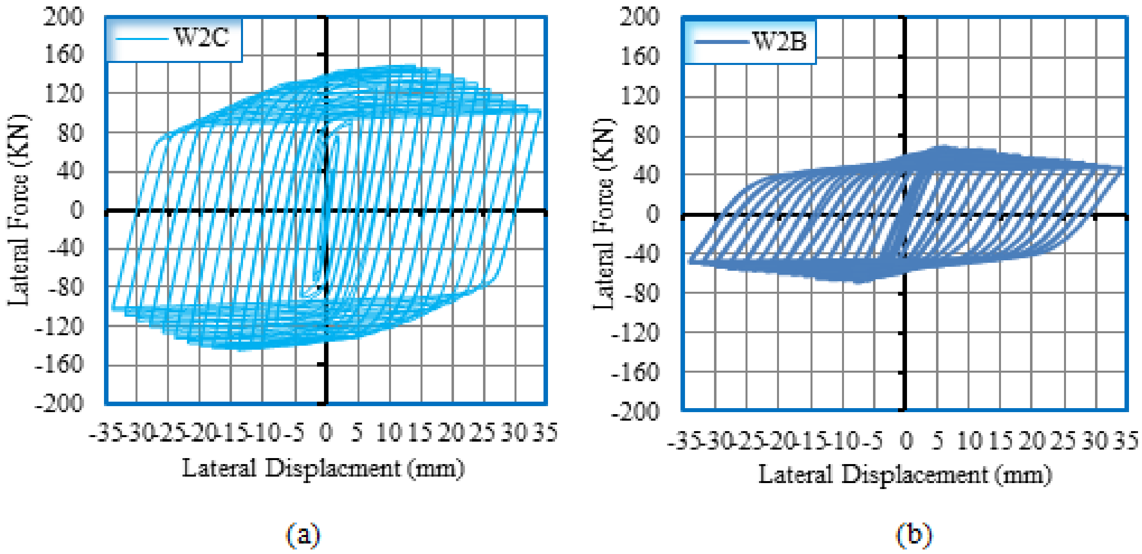

Figure 4-13 Hysteresis curve of reinforced and unreinforced masonry wall

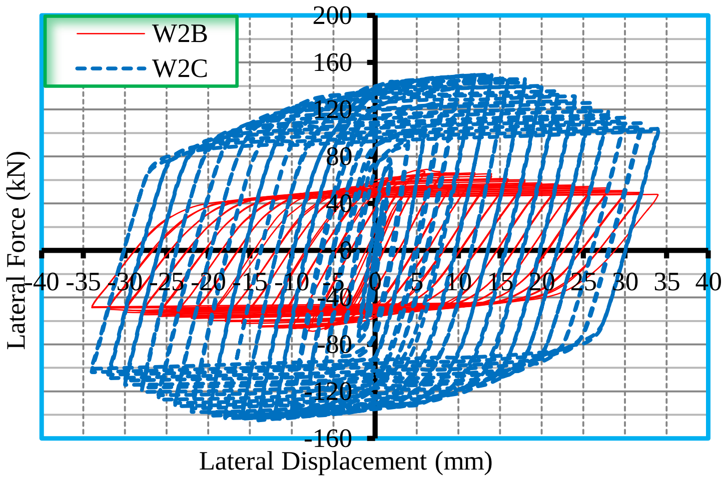

Figure 4-14 Comparison hysteresis curve of reinforced and unreinforced RMs

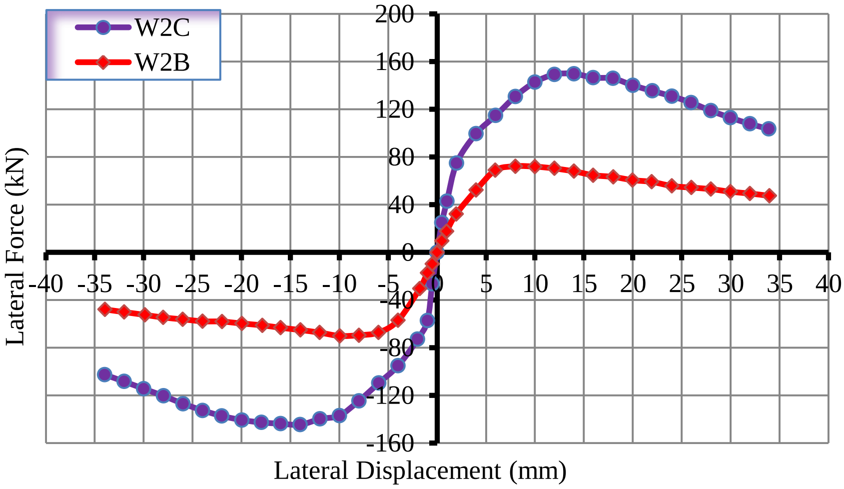

Figure 4-15 Comparison envelop hysteresis curve of reinforced and unreinforced RMs

The effect of using reinforcement on the seismic performance of masonry walls with the same aspect ratio was presented in Table 4-7 above. A comparison made based on force-displacement relation and secant stiffness and lateral displacement relation between reinforced HCB fully grouted masonry wall and unreinforced HCB fully grouted masonry wall is shown in Figure 4-13 to Figure 4-16. and its comparison of enveloping ultimate force- lateral displacement of two modeled walls show in figure 4-15 and Table 4-8.

Table 4-8 Reinforcement use in wall comparison for aspect ratio 1.95 wall, the horizontal reinforcement ratio 0.13% and vertical reinforcement ratio 0.65%

Wall ID	PU				Ductility			
	Push (kN)	Amplification %	Pull (kN)	Amplification %	push	Amplification (%)	pull	Amplification (%)
W2B	72.21	----	-70.11	----	2.53		2.59	
W2C	149.78	51.79	-144.59	51.51	1.92	-31.18%	2.07	-25.12%

The result shows that the ultimate strength of the unreinforced HCB fully grouted masonry walls are 72.21 kN and 70.11 kN and 149.78kN and 144.59kN for reinforced HCB fully grouted masonry wall in the push and pull directions respectively. As it can be seen from the results shear resistance of reinforced HCB fully grouted masonry walls is higher in a push and pulls direction by 51.79% and 51.51% than that of unreinforced HCB fully grouted masonry walls. The result shows reinforcement has a favorable influence on the shear strength of walls or the unreinforced masonry wall.

In Table 4.8, the reduction of 31.18% for push and 25.12% for pull direction in ductility was recorded when the wall modeled reinforced masonry, where horizontal reinforcement Ø10@c/c400mm and vertically reinforcement Ø16@c/c200mm used. This result show reinforcement used in HCB grouted masonry wall is a significant influence on the ductility of a wall, This shows reinforced HCB fully grouted masonry wall is high seismic resistance than unreinforced HCB fully grouted masonry wall, also the displacement ductility of reinforced HCB fully grouted masonry wall smaller than unreinforced HCB grouted masonry wall.

Stiffness degradation curve

Stiffness degradation refers to the phenomena that the displacement of a structure increases with an increase of applied time of the same load. Secant stiffness is calculated using the following equation (Qiang Z. et al., 2020)

$$Ki=\frac{|-Pi|+|+Pi|}{|-Xi|+|+Xi|}$$ --Equation 4.2

Where Ki is secant stiffness

-Pi and +Pi are peak load in the forward and downward loading process

-Xi and +Xi are peak displacement in the forward and downward loading process.

In stiffness curve, the abscissa represents the horizontal displacement and the ordinate represents the ratio of secant stiffness.

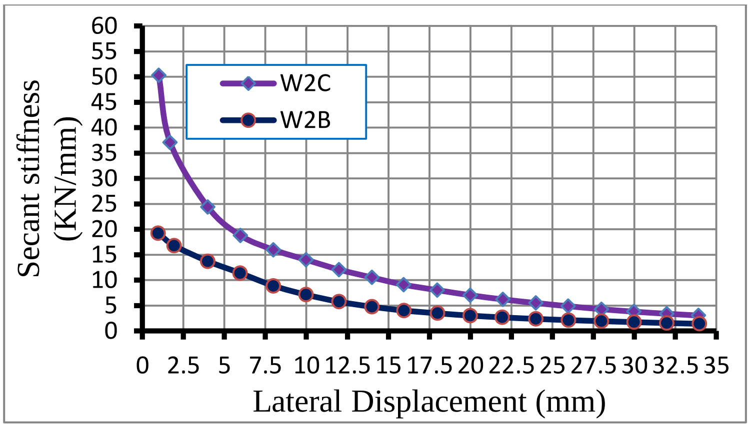

Figure 4-16 Stiffness degradation comparison of reinforced and unreinforced masonry wall of aspect ratio 1.95

From the above Figure 4.16, the stiffness degradation of W2C is higher than the stiffness degradation of W2B. This result show reinforcement use in a wall is advantageous to improve the stiffness walls.

4.3.3. Effect of reinforcement spacing on masonry seismic performance

4.3.3.1. Effect of vertical reinforcement Spacing on masonry strength

In this parametric study, two cases were considered in the first case spacing and diameters of vertical reinforcements are 400mm and Ø16mm respectively, and in the second case 200mm and Ø16mm. The spacing and the diameter horizontal reinforcements (Ø10mm@c/c400mm) are similar for both cases. Because of the change spacing of the vertical reinforcement, the vertical reinforcement ratio also changes from 0.37% to 0.65%, and the wall aspect ratio (H/L) is 1.39.

Table 4-9 Matrix of a studied reinforced masonry wall with different vertical reinforcement spacing

wall ID	aspect ratio (H/L))	Reinforcement dimension		Reinforcement C/C spacing		Grouted Type
		horizontal	vertical	horizontal	vertical	
W1C	1.39	Ø10mm	Ø16mm	400mm	200mm	Fully
W1D	1.39	Ø10mm	Ø16mm	400mm	400mm	Fully

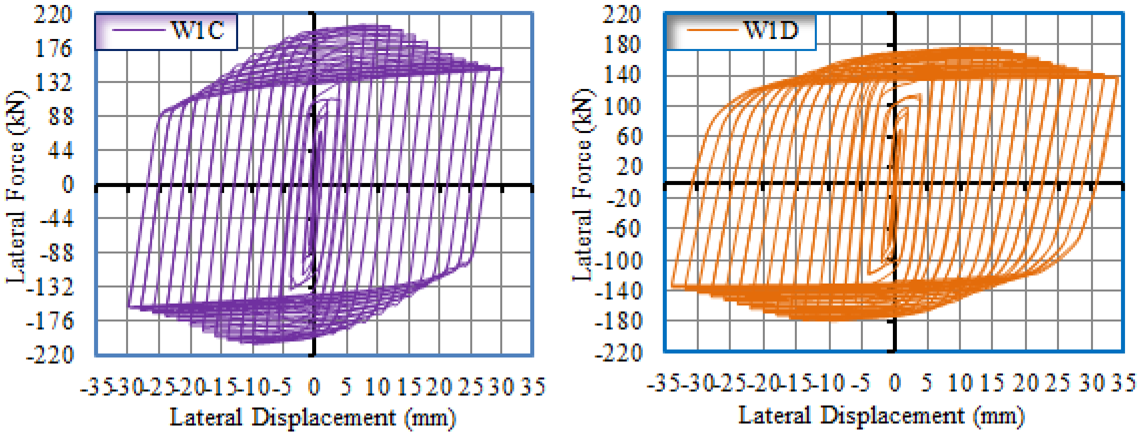

a) Vertical reinforcement spacing 200mm b) Vertical reinforcement spacing 400mm

Figure 4-17 Hysteresis Curve of RMW with different vertical reinforcement spacing

The Ultimate load resistance of the two walls was a comparison, and the percentage amplification of carrying capacity of the walls was shown in below figure 4.18, figure 4-19, and table 4.10. The reinforced HCB fully grouted masonry wall aspect (H/L) ratio is 1.39, and its material property is similar. Also, the spacing and dimension of horizontal reinforcement of both two models are similar arrangements but, vertical reinforcement is similar in diameter and different spacing.

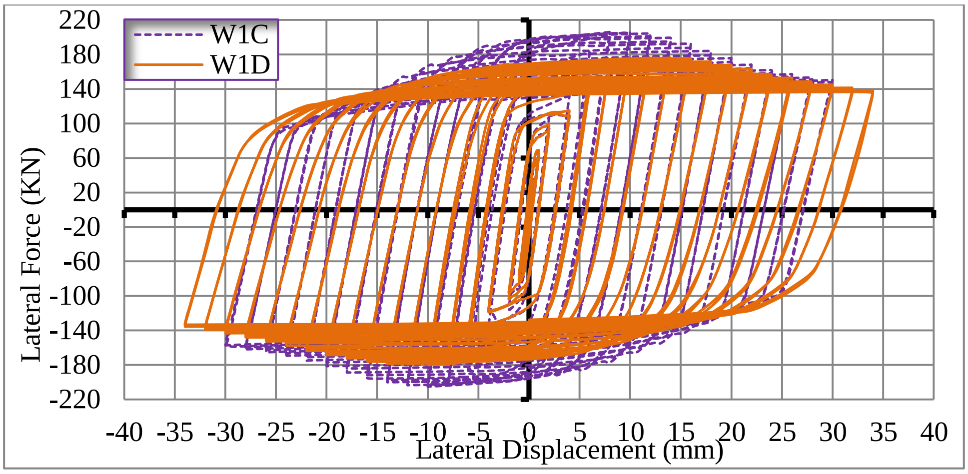

Figure 4-18 Comparison hysteresis curve of RMW with different vertical reinforcement spacing

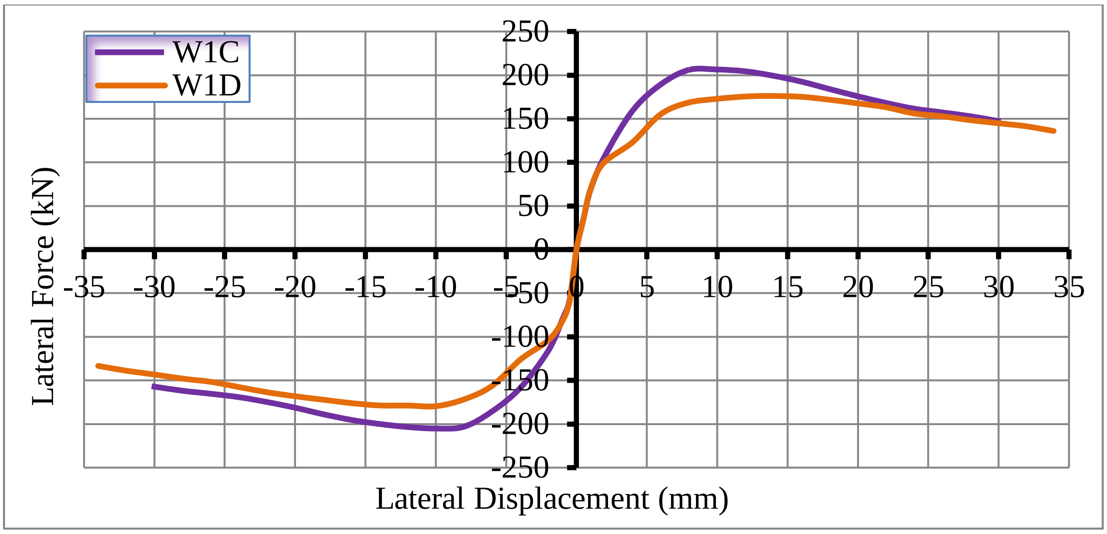

Figure 4-19 Comparison hysteresis envelop curve of RMW with different vertical reinforcement spacing

The shear resistance of the wall with vertical reinforcement of Ø16mm@c/c200mm is 206.521kN for push and 205.15kN for pull directions, and 176.192kN for push and 179.56 kN for pull directions for the wall with vertical reinforcement of Ø16mm@c/c400mm.

Table 4-10 Comparison of the effect of vertical reinforcement spacing of wall aspect ratio 1.39

Wall ID	C/C spacing of reinforcement		PU			
	Horizontal	Vertical	Push (kN)	Amplification %	Pull (kN)	Amplification %
W1C	Ø10@c/c400mm	Ø16@c/c200	206.521	----	-205.15	----
W1D	Ø10@c/c400mm	Ø16@c/c400	176.192	-17.21	-179.56	-14.25

Based on the above Table 4.10, the ultimate shear resistance of the wall is reduced by 17.21% for push and 14.25% for pull direction for in-plane load when the spacing of Ø16 vertical reinforcement increases from 200mm to 400mm. This indicates that when the spacing of vertical reinforcement increases the shear resistance decreases or the spacing of vertical reinforcement has a significant role in the shear resistance of walls.

4.3.3.2. Effect of horizontal reinforcement spacing on masonry strength

In this part, the effect of the horizontal reinforcement ratio is investigated. To see its effect, the aspect (H/L) ratio and vertical reinforcement ratio (0.65%) are kept the same. In this study the diameter and spacing of vertical reinforcement are Ø16mm@c/c200mm, The two cases differ with horizontal reinforcement diameter and spacing. For the first case, horizontal reinforcement diameter and spacing are Ø10mm@c/c400mm and for the second case, horizontal reinforcement diameter and spacing are Ø10mm@c/c200mm.

Table 4-11 Matrix of a studied reinforced masonry wall with different horizontal reinforcement spacing

wall ID	aspect ratio (H/L))	Reinforcement dimension		Reinforcement C/C spacing		Grouted Type
		vertical	horizontal	vertical	horizontal	
W1C	1.39	Ø16mm	Ø10mm	200mm	400mm	Fully
W1E	1.39	Ø16mm	Ø10mm	200mm	200mm	Fully

The hysteretic skeleton curves of the model walls aspect (H/L) 1.39 are presented in Figure 4.20, and also the comparison of the enveloping curve of the model reinforced masonry wall is presented in Figure 4.21. The wall vertical reinforcement ratio and spacing are similar, but the horizontal reinforcement spacing and dimension for wall W1C are Ø10mm@c/c400mm, and W1E are Ø10mm@c/c200mm.

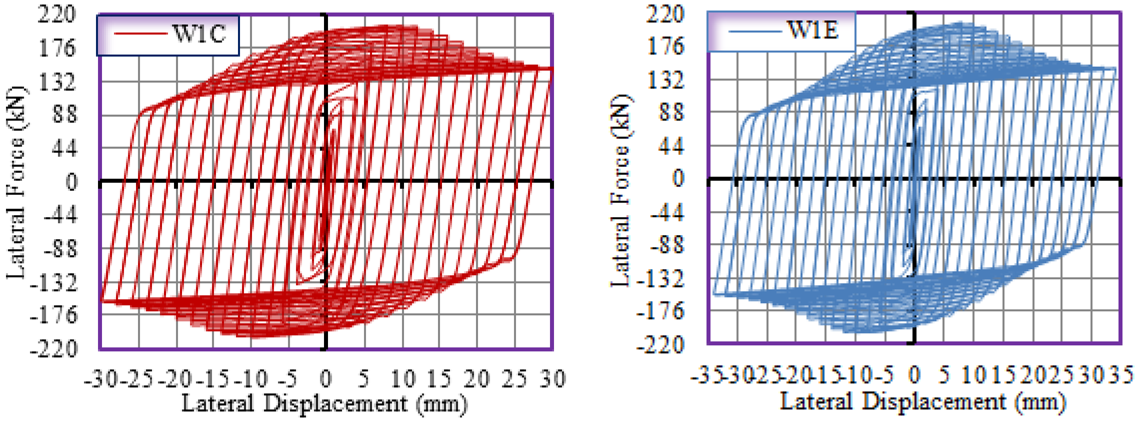

Figure 4-20 Hysteresis curve of RMW with different horizontal reinforcement spacing

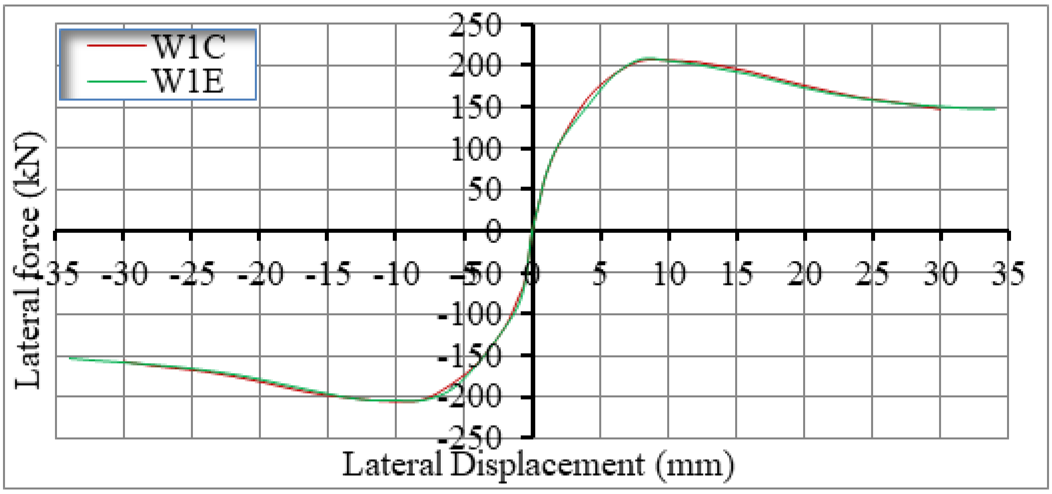

Figure 4-21 Comparison hysteresis envelop curve of RMW with different horizontal reinforcement spacing

Table 4-12 Comparison effect of horizontal reinforcement spacing of wall aspect ratio 1.39

Wall ID	Spacing of reinforcement		Pu			
	vertical (mm)	horizontal (mm)	Push (kN)	Amplification %	Pull (kN)	Amplification %
W1E	Ø16@c/c200mm	Ø10@c/c200	207.882	---	-204.017	---
W1C	Ø16@c/c200mm	Ø10@c/c400	206.521	-0.659%	-204.001	0.008%

Table 4.12 that the ultimate load resistance of the wall is reduced by 0.569% for push and 0.008% for pull directions for in-plane load when the spacing of Ø10 vertical reinforcement increases from 200mm to 400mm. This result indicates that the spacing of horizontal reinforcement has a minor effect on the ultimate load strength of the walls, this means horizontal reinforcement becomes negligible at high values of wall aspect ratio because the shear wall will be more characterized by flexural deformations.

4.3.4. Effect of vertical Reinforcement ratio variation on reinforced masonry wall under the seismic effect

In this, study the horizontal reinforcement ratio is constant, but the vertical reinforcement ratio is variable (0.26%, 0.36%, and 0.65%), the reinforcement ratio varies due to different reinforcement diameters 10mm, 12mm, and 16mm respectively.

Table 4-13 Matrix of a studied reinforced masonry wall with different horizontal reinforcement spacing

Wall ID	Aspect ratio	Horizontal reinforcement dimension	Vertical reinforcement dimension	Horizontal reinforcement ratio	Vertical reinforcement ratio
W1F	1.39	Ø10mm@c/c400mm	Ø10mm@c/c200mm	0.13%	0.26%
W1G	1.39	Ø10mm@c/c400mm	Ø12mm@c/c200mm	0.13%	0.36%
W1H	1.39	Ø10mm@c/c400mm	Ø16mm@c/c200mm	0.13%	0.65%

The vertical and horizontal reinforcements used in walls W1F, W1G, and W1C are Ø10mm@c/c200mm and Ø10mm@c/c400mm, Ø12mm@c/c200mm and 10mm@c/c400mm, and Ø16mm@c/c200mm and Ø10mm@c/c200mm respectively.

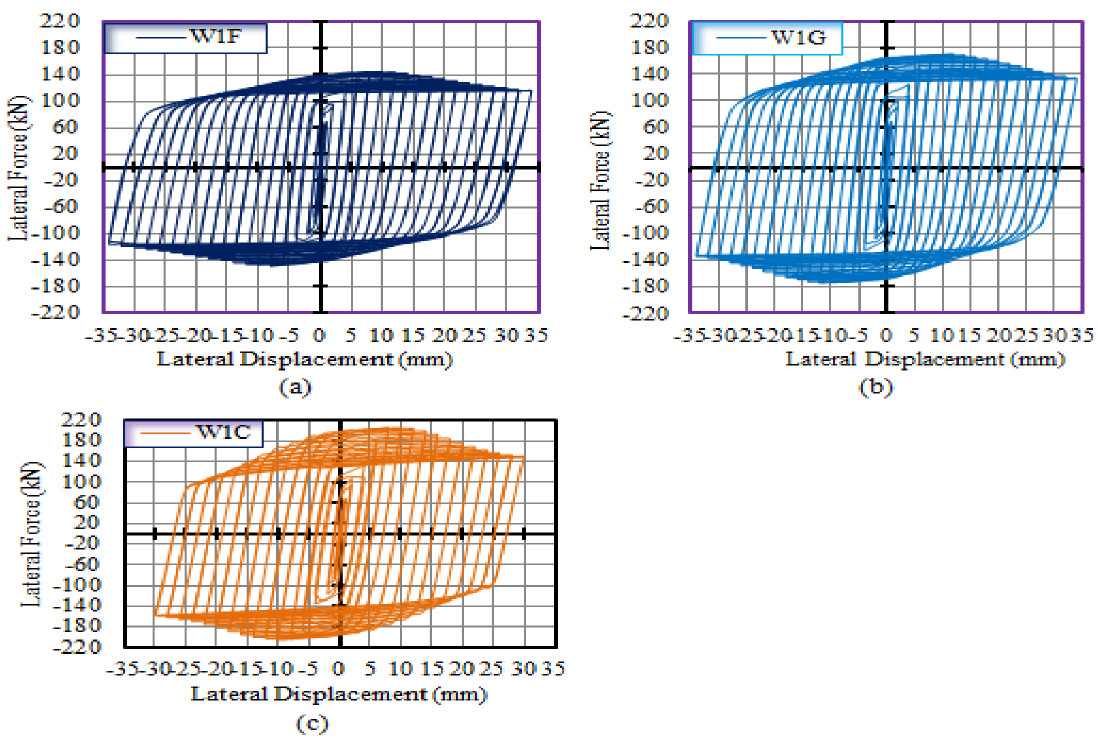

Figure 4-22 hysteresis curve of RMW with different vertical reinforcement ratio

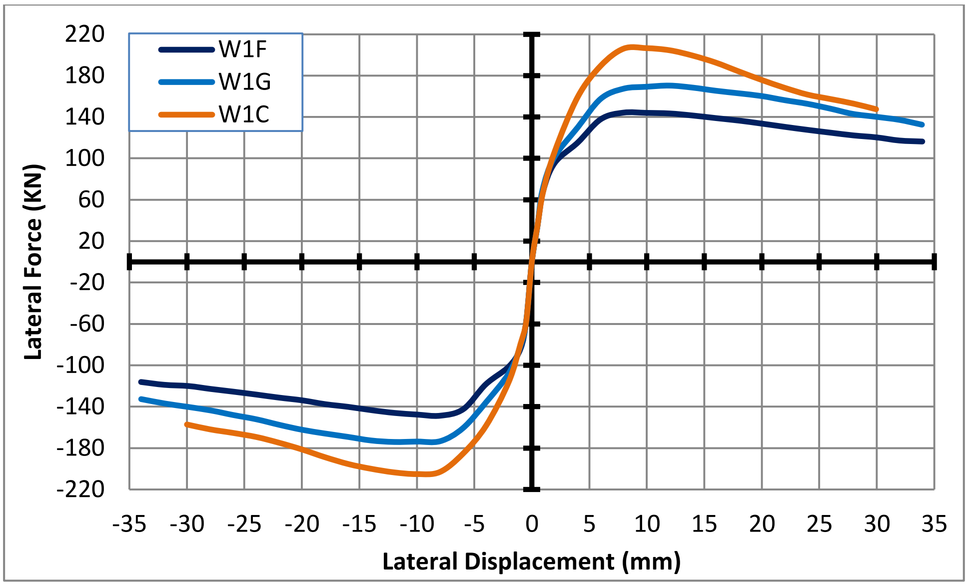

Figure 4-23 Hysteresis envelop curve of RMW with different vertical reinforcement ratio

From table 4-14, the ultimate shear resistances in push and pull directions for W1F are 144.2kN and 148.725kN, for W1G are also 170.337kN and 174.107kN and for W1C 206.52kN and 204.151kN respectively, generally its ultimate resistance and comparison show in below table 4.14.

Table 4-14 Comparison of the effect of vertical reinforcement ratio of wall aspect ratio 1.39

Wall ID	Aspect (H/L) ratio	PU				ductility	
		Push (kN)	Amplification %	Pull (kN)	Amplification %	push	pull
W1F	1.39	144.2	----	148.725	----	2.239	2.241
W1G	1.39	170.34	15.344%	174.107	14.578%	2.181	2.195
W1C	1.39	206.52	30.176%	204.151	27.149%	2.1653	2.1642

Above Figure 4-22 and Table4.14, Show that the ultimate load resistance of walls differs due to changing vertical reinforcement ratio. The Ultimate load resistance of W1G for push and pull directions are higher than that of W1F by 15.344% and 14.578%, respectively. Also, the Ultimate load resistance of W1C for Push and Pull directions are higher than that of W1F by 30.176% and 27.149% respectively; this result shows vertical reinforcement ratio has a significant effect on the ultimate load capacity of walls.

4.3.5. Effect of vertical reinforcement spacing on the same reinforcement ratio of masonry wall

In this study, the vertical reinforcement ratio of the wall is constant 0.37% but, the spacing of the vertical reinforcements was variable for W1I Ø6mm@c/c200mm, and W1D Ø16mm@c/c400mm, the horizontal reinforcement ratio and spacing are constant or Ø10mm@c/c400mm. Generally, the study masonry wall geometry has presented in Table 4-15 below.

Table 4-15 Matrix of a studied reinforced masonry wall with different vertical reinforcement spacing on the same reinforcement ratio

wall ID	aspect ratio (H/L)	Reinforcement ratio	Reinforcement dimension		Reinforcement C/C spacing		Grouted Type
			Horizontal	vertical	horizontal	vertical	
W1D	1.39	0.37%	Ø10mm	Ø16mm	400mm	400mm	Fully
W1I	1.39	0.37%	Ø10mm	Ø6mm	400mm	200mm	Fully

The ABAQUS result generally present in the following table and figure the loading applied on the wall 1MPa because of top-loading beam.

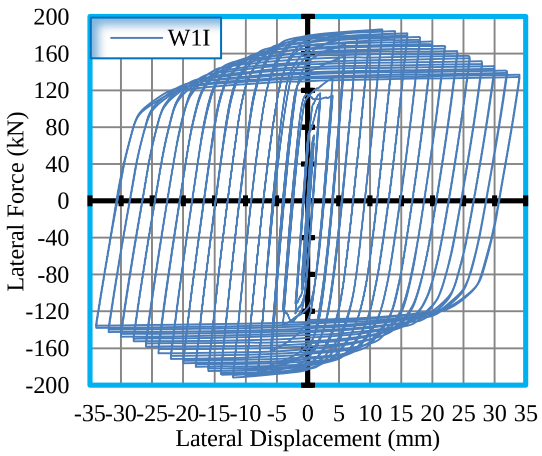

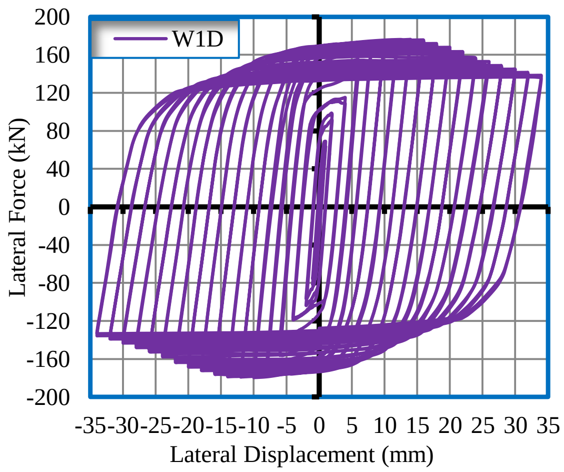

Figure 4-24 Hysteresis curve of RMW with different vertical reinforcement spacing without change vertical reinforcement ratio

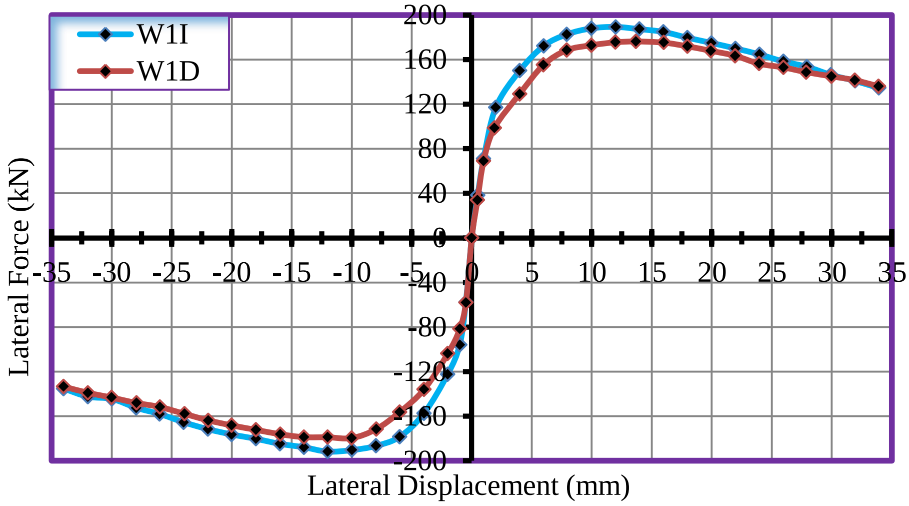

Figure 4-25 Hysteresis envelop curve of RMW with different vertical reinforcement spacing without change vertical reinforcement ratio

From above, Figure 4-23 and Figure 4-24, the ultimate shear capacity of wall W1D or the vertical reinforcement Ø6mm@c/c200mm is 189.265kN and 191.1kN for push and pull direction respectively, also wall W1I or the vertical reinforcement Ø16mm@c/c400mm is 176.192kN and 179.56 for, push and pull direction respectively. But the vertical reinforcement ratio, horizontal reinforcement geometry, and spacing are constant.

Table 4-16 Comparison result of wall vertical reinforcement spacing variation on the same reinforcement ratio

Wall ID	Vertical reinforcement		Horizontal reinforcement		Ultimate load		Amplification	
	ratio	spacing	ratio	spacing	push	pull	Push%	Pull%
W1D	0.37%	400mm	0.13%	400mm	176.19	179.56	….	…..
W1I	0.37%	200mm	0.13%	400mm	189.26	191.1	7.42%	6.43%

Table 4-16 shows the ultimate load capacity of W1I for push and pull directions are higher than that of W1D by 7.42% and 6.43%, respectively, because of change the spacing of reinforcement from 400mm to 200mm, but the reinforcement ratio does not change. This result show closed spaced reinforcement wall is high strength than a separate spaced reinforcement wall. It can be observed that providing vertical reinforcement with close spacing enhances the ultimate load capacity.

5. CONCLUSION AND RECOMMENDATION

5.1. Conclusion

The in-plane behavior of unreinforced HCB fully grouted and reinforced HCB fully grouted masonry walls with different aspect (H/L) ratio, vertical and horizontal reinforcement spacing has been studied under cyclic loading in quasi statics method. Based on the finite element analysis result and discussion of reinforced and unreinforced fully grouted masonry walls are the following remarks are outlined.

1. The modeling of reinforced and unreinforced HCB fully grouted masonry wall in ABAQUS by simplifying micro model result is in good agreement with the experimental results.
2. The wall aspect ratio 1.95 or high aspect ratio reinforced fully grouted and unreinforced masonry wall comparison, the unforced masonry wall easily fail because the HCB units rapidly separate each other. A reinforced masonry wall is ultimate in-plane load, resistance of more than 51.79% of the ultimate load resistance of an unreinforced masonry wall. This shows reinforced HCB fully grouted masonry wall is higher seismic resistance than unreinforced HCB fully grouted masonry walls. Generally reinforcement use in walls great advantageous to improve the ultimate strength of the wall.
3. Increase the wall aspect ratio (H/L) from 1.39 to 2.23 has a significant influence on the shear strength at the same reinforcement distribution and axial compression stress on the wall. Due to the aspect (H/L) ratio variation the seismic resistance and failure type of wall was changed. Aspect ratio increases the seismic resistance of the wall decrease, if the aspect ratio increase the wall fails because of flexure.
4. In the reinforced HCB fully grouted masonry wall seismic resistance reinforcement spacing and the ratio was a significant role. The spacing of vertical reinforcement increases the ultimate strength of the wall decrease. But the spacing of horizontal reinforcement increase or decrease the ultimate strength of wall changes with a small difference. For in-plane load the role of vertical reinforcement is higher than the role of horizontal reinforcement. This represents horizontal reinforcement has a minor effect on the ultimate strength of the wall or horizontal reinforcement becomes

negligible at high values of wall aspect ratio since the shear wall will be more characterized by flexural deformations.

5. Vertical reinforcement in the wall is a significant role in masonry strength and stiffness, vertical reinforcement closed spaced the ultimate strength enhances, without change the vertical reinforcement ratio.
6. The wall stiffness of aspect ratio 1.39 is higher than aspect ratio 1.95; i.e. as the aspect ratio increases the wall initial stiffness decrease.

5.2. Recommendation

For seismic affected site masonry building is constructing by reinforced HCB fully grouted masonry effectively resist the seismic load. Because reinforcement uses in walls highly increase the ultimate strength of walls relative to unreinforced HCB fully grouted masonry wall.

For long highest unreinforced un-fill wall building is fail because of low vibration or seismic load, but reinforcement used in these walls highly improves its ultimate strength and stiffness.

To fill the gap of this study the following recommendations are suggested for future researchers:

- The development of the finite element model in this study was limited by computer, i.e., the model needed only to be sophisticated enough to provide the basic information needed for design purposes. However, a more sophisticated model taking into consideration the three-dimensional nature of the problem, especially when the fully grouted masonry wall axis, the nonlinear characteristics of the different elements such as mortar, masonry, grout, and the cyclic nature of the loading, could all be further investigated.

REFERENCE

ABAQUS. *manual.* USA: Dassault systemes Simulia Cro , providence,RI, 2016.

ACI Committee, 318. *Building Code Requirements for Structural Concrete ,ACI 318-01.* Farmington Hills, MI, USA,: American Concrete Institute, 2014.

Alcocer, S.M. and Klinger, R.E. "Masonry Research in the Americas." *Masonry in the Americas, American Concrete Institute*, 1994: SP-147, pp. 127-169.

ASTM. "Specification for Hydrated Lime for Masonry Purposes." *ASTM C207- 1999, West Conshohocken, Pa*, 1999.

ASTM, E 519-02. "Standard test method for diagonal tension (shear) in masonry assemblages. ASTM standards, Philadelphia." 2002.

Drysdale, R. G., Hamid, A. A., and Baker, L. R. " Masonry structures: Behaviour and design, Prentice-Hall, Englewood Cliffs, N.J." 1994.

ES, EN 1992-1-1. *Design of Concrete structure Ethiopian standards.* addis abeba: Ethiopian standards Revision Committee, December 2015.

ES, EN 1996-1-1. *Design of masonry structure.* addis abeba: Ethiopian standards Revision Committee, December 2015.

Fattal, S.G. and Cattaneo, L.E. "Evaluation of Structural Properties of Masonry in Existing Buildings, National Bureau of Standards, Department of Commerce, Washington." 1977.

FEMA, (Federal Emergency ManagementAgency). "Damage states and fragility curves for reinforced masonry shear walls." *FEMA P-58/BD-3.8.10,* Washington, USA; 200.

FEMA, (Federal Emergency ManagementAgency). "Interim testing protocols for components." *FEMA, Washington, USA*, Report No. 461; 2007.

G. Vasconcelos, P. Lourenço, C. Alves, J. Pamplona and T. Miranda. " Relation between tensile and compressive engineering properties of granites ." *Harmonising Rock Engineering and the Environment. Taylor & Francis Group,* 2012: 867-872.

Hany Mohamed, Seif Eldin. "In-plane shear behavior of fully grouted reinforced masonry shear walls. Ph.D. Thesis, department of Building, Civil and Environmental Engineering, Concordia University." 2016.

Hsu, T. C. and Mo, Y. L. "Unified Theory of Concrete Structures." *John Wiley, UK*, 2010.

J.G, Rots. "Computational modeling of concrete fracture." *Doctoral Thesis, Delft University of Technology, Netherlands*, 1988.

Kurdo F Abdulla, Lee S. Cunningham, Martin Gillie. "Simulating masonry wall behaviour using a simplified micro-model approach." *Mechanical, Aerospace and Civil Engineering School, The University of Manchester, Oxford Road, Mancheste*, 2017: 351-356.

Lourenço, P. B. "Computational strategies for masonry structures." *PhD Thesis. Delft University Press, Delft*, 1996.

Lourenço, Paulo B. "Masonry Modeling." *International Journal of Advanced Engineering Research and Technology*, 2014.

M. Angelillo, P. B. Lourenço and G. Milani. " masonry behaviour and modelling." *MEchanics of masonry structures. Springer, pp. 1-26, 2014*, 2014: 1-26.

Marzhan, G. "The Shear Strength of Dry-Stacked Masonry Walls." *Institüte fürMassivbau und Baustofftechnologie, Universität Leipzig*, 1998.

Park, R. "Evaluation of ductility of structures and structural assemblages from laboratory testing." *Bulletin of the New Zealand National Society for Earthquake Engineering*, (1989): Vol 22, No. 3,pp.155-166.

Pauley, T. & Priestly, M.J.N. " Seismic design of reinforced concrete and masonry buildings." *John Wiley & Sons, Inc*, 1992.

Qiang Zhou, Lingyu Yang, and Wenyang Zhao. "Experimental Analysis of Seismic Performance of Masonry Shear." *School of Civil Engineering and Architecture, Nanchang University, Nanchang 330031, China*, 2020: Volume 2020, Article ID 4015790, 13 pages.

Seif ElDin, H. M., and Galal, K. "Influence of Axial Compressive Stress on the In-Plane Shear Performance of Reinforced Masonry Shear Walls." *11th Canadian Conference on Earthquake Engineering, Victoria, BC, Canada*, 2015.

Seif ElDin, H. M., and Galal, K. "Survey of Design Equations for the In-Plane Shear Capacity of Reinforced Masonry Shear Walls." *12th North American Masonry Conference Denver, Colorado*, 2015.

Wahalathantri, Buddhi Lankananda,Thambiratnam,d,p, Chan, T.H.T., and Fawzia, S. "A Material Model for Flexural Crack Simulation in reinforced Concrete Elements using ABAQUS." *Infrastructure Transport and Urban Development*, 2011: 260-264.

Yunus, Dere and Mehmet,Alpaslan,Koroglu. "Nonlinear FE Modeling of Reinforced Concrete." *International Journal of Structural and Civil Engineering Research*, February 2017: Vol. 6, No. 1.

APPENDIX A

Aspect ratio variation

A. Length of wall 1435mm, thickness of wall 150mm but the height of wall is variable

Fully grouted reinforced masonry wall horizontal reinforcement bar Ø10@400mm and vertical reinforcement bar Ø16@200mm, horizontal and vertical reinforcement ratio is 0.13% and 0.65%reispactively

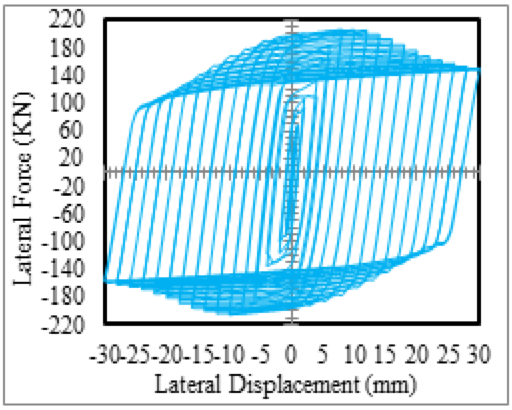

a

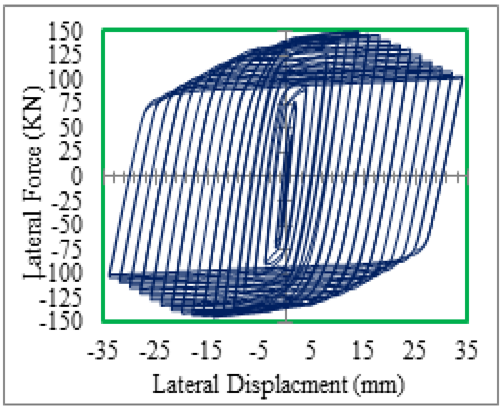

b

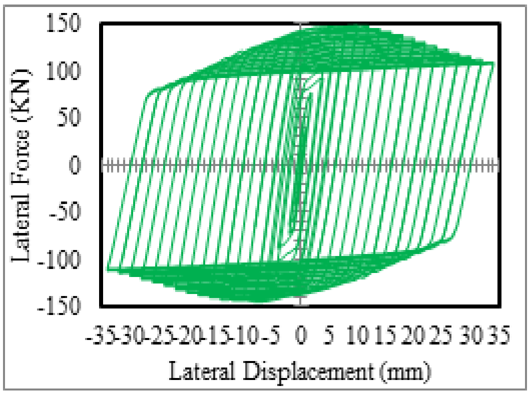

c

Figure A.1 hysteresis curve of wall a) W1C, b) W2C and c) W3C

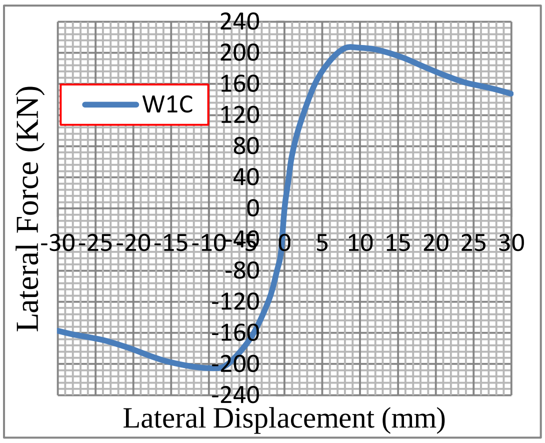

a

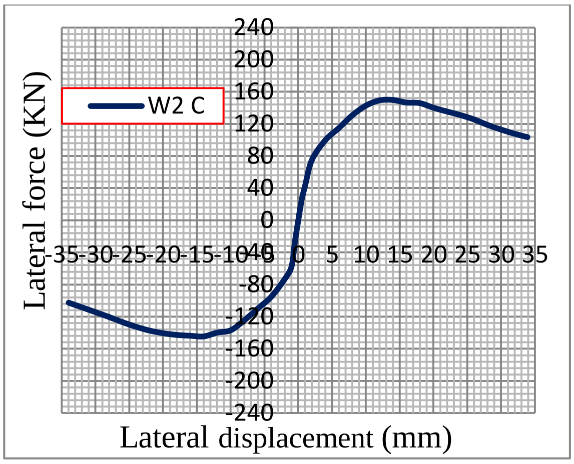

b

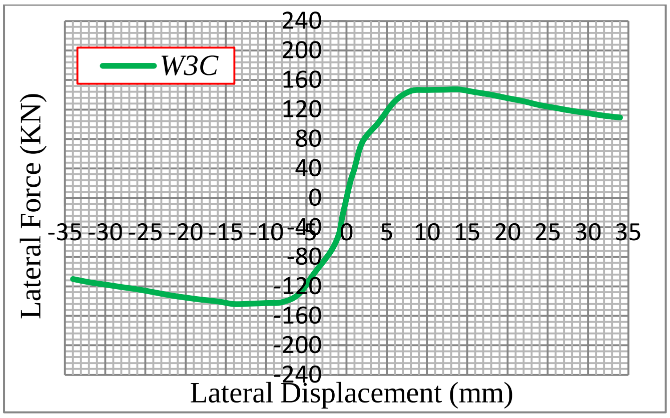

c

Figure A.2 hysteresis envelop curve of Wall, a) aspect ratio 1.39, b) aspect ratio 1.95 and c) aspect ratio 2.23

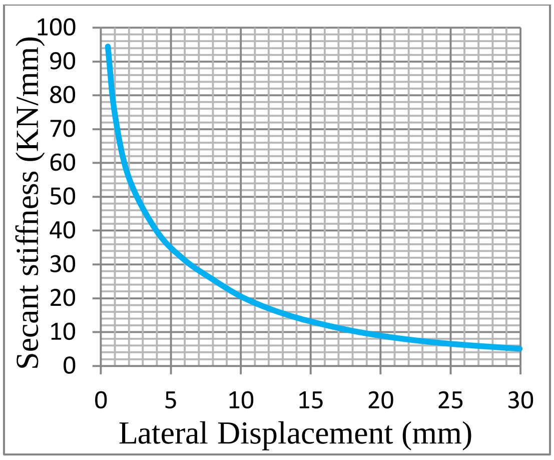

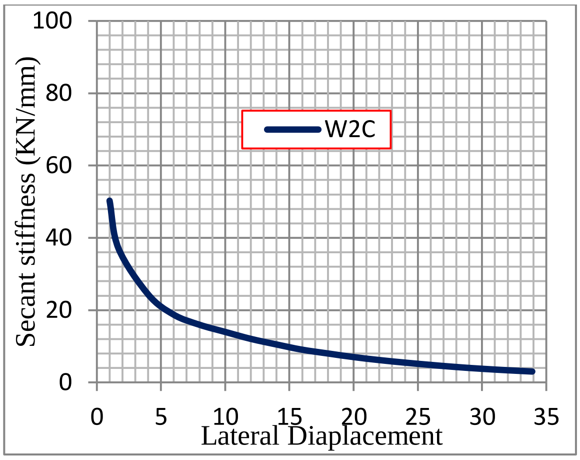

a

b

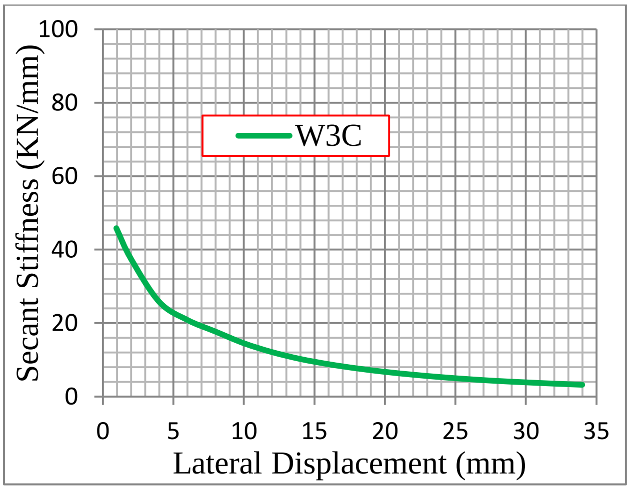

c

Figure A.3 Stiffness degradation of masonry wall, a) aspect ratio 1.39, b) aspect ratio 1.95 and c) aspect ratio 2.23

APPENDIX B

Vertical reinforcement spacing variation

A. In wall model aspect ratio 1.39 use Vertical reinforcement Ø16@400mm and Ø16@400mm and but horizontal reinforcement Ø10@400mm both case

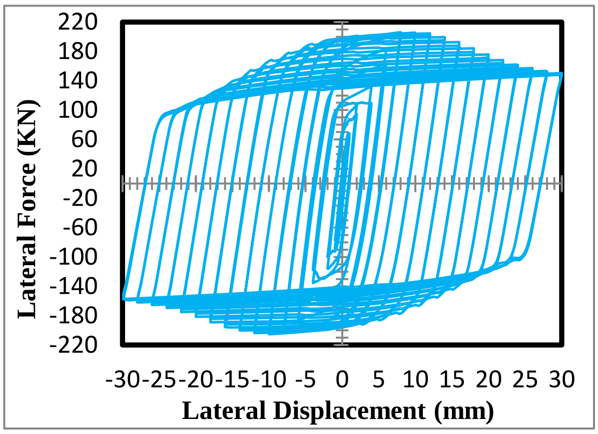

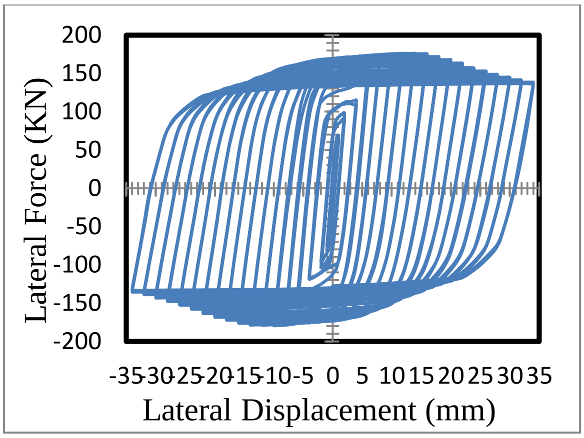

b

Figure B.1 hysteresis curve of reinforced masonry wall 1, a) vertical reinforcement Ø16@200mm b) vertical reinforcement Ø16@400mm

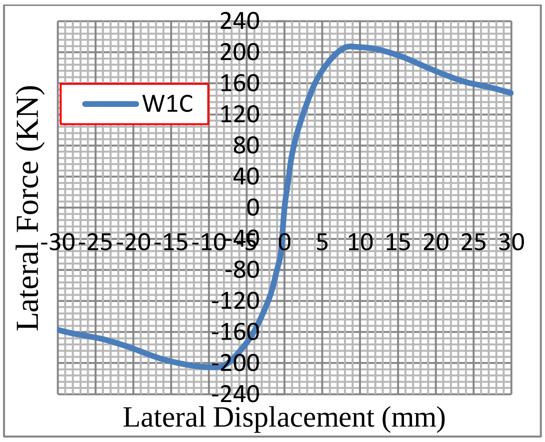

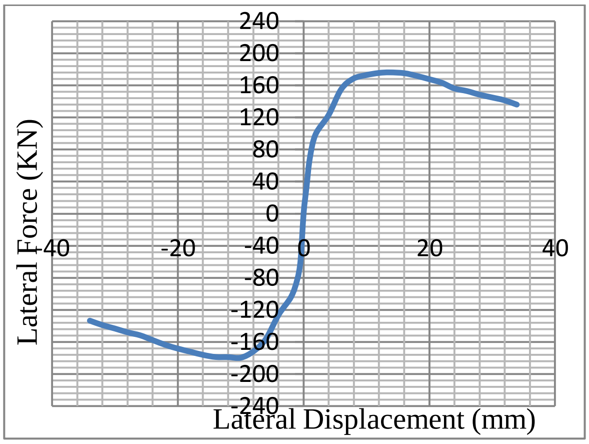

a

b

Figure B.2 hysteresis envelop curve of reinforced masonry wall, a) vertical reinforcement Ø16@200mm b) vertical reinforcement Ø16@400mm

APPENDIX C

Horizontal Reinforcement Spacing Variation

A. In wall model aspect ratio 1.39 use Vertical reinforcement the same Ø16@400mm and but horizontal reinforcement Ø10@400mm and Ø10@200mm both case.

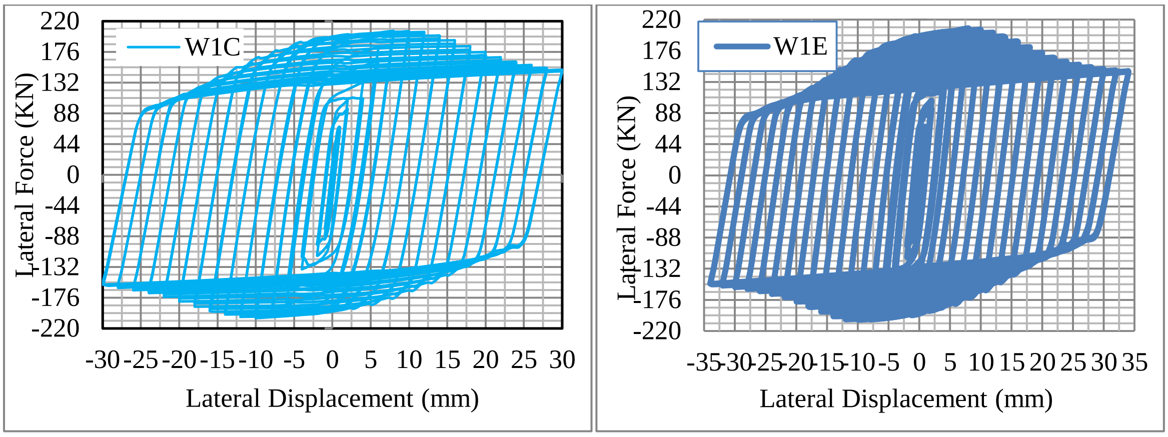

a b

Figure C.1 hysteresis curve of reinforced masonry wall 1, a) horizontal reinforcement Ø10@400mm b) horizontal reinforcement Ø10@200mm

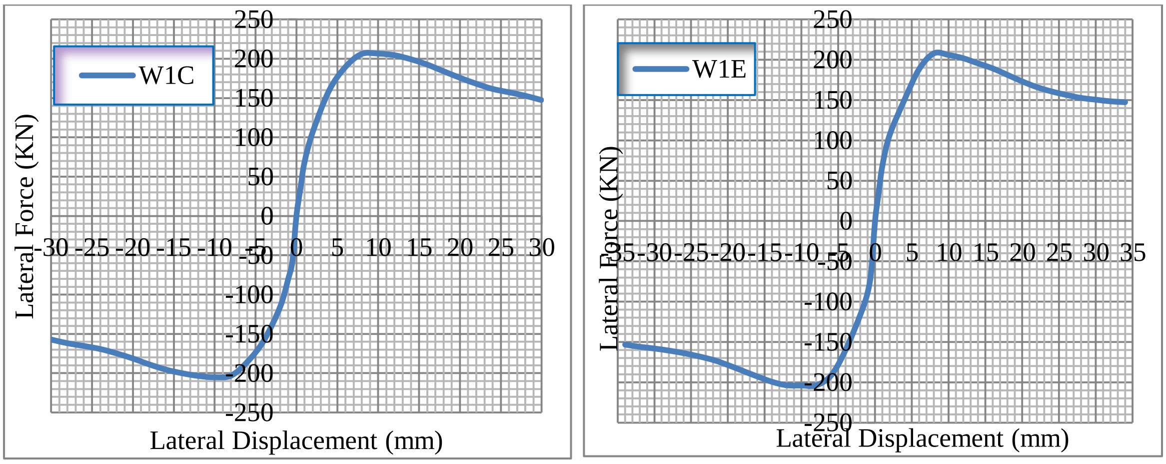

a b

Figure C.2 hysteresis envelop curve of reinforced masonry wall, a) horizontal reinforcement Ø10@400mm b) horizontal reinforcement Ø10@200mm

APPENDIX D

Failure patterns of masonry wall

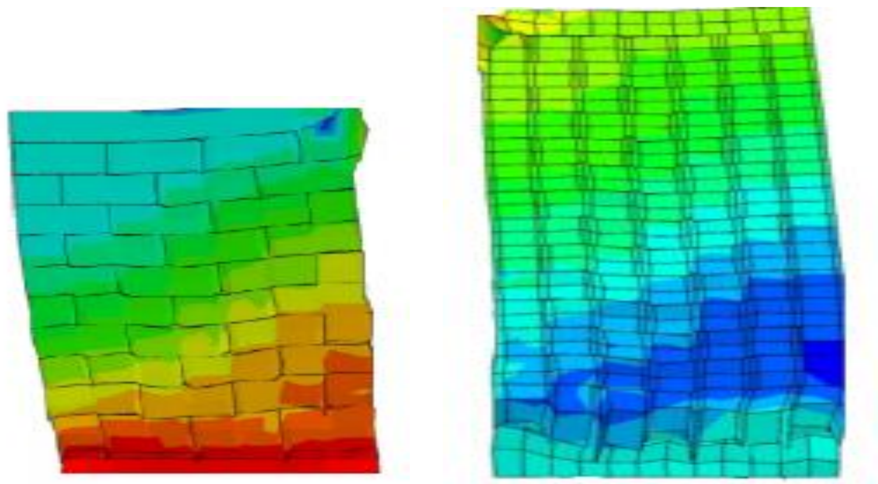

(a) (b)

Figure D1 Failure pattern of masonry wall at displacement 7.3mm (a), aspect ratio 1.39 (b), aspect ratio 2.23